

1-1-2007

## Thermal hydraulic analysis of the High-Power Race Target

Ryan D LeCounte

*University of Nevada, Las Vegas*

Follow this and additional works at: <https://digitalscholarship.unlv.edu/rtds>

---

### Repository Citation

LeCounte, Ryan D, "Thermal hydraulic analysis of the High-Power Race Target" (2007). *UNLV Retrospective Theses & Dissertations*. 2247.

<http://dx.doi.org/10.25669/dcs5-j59n>

This Thesis is protected by copyright and/or related rights. It has been brought to you by Digital Scholarship@UNLV with permission from the rights-holder(s). You are free to use this Thesis in any way that is permitted by the copyright and related rights legislation that applies to your use. For other uses you need to obtain permission from the rights-holder(s) directly, unless additional rights are indicated by a Creative Commons license in the record and/or on the work itself.

This Thesis has been accepted for inclusion in UNLV Retrospective Theses & Dissertations by an authorized administrator of Digital Scholarship@UNLV. For more information, please contact [digitalscholarship@unlv.edu](mailto:digitalscholarship@unlv.edu).

THERMAL HYDRAULIC ANALYSIS OF THE  
HIGH-POWER RACE TARGET

by

Ryan D. LeCounte

Bachelor of Science  
University of Nevada, Las Vegas  
2006

A thesis submitted in partial fulfillment  
of the requirements for the

**Master of Science Degree in Materials and Nuclear Engineering  
Department of Mechanical Engineering  
Howard R. Hughes College of Engineering**

**Graduate College  
University of Nevada, Las Vegas  
December 2007**

UMI Number: 1452259

### INFORMATION TO USERS

The quality of this reproduction is dependent upon the quality of the copy submitted. Broken or indistinct print, colored or poor quality illustrations and photographs, print bleed-through, substandard margins, and improper alignment can adversely affect reproduction.

In the unlikely event that the author did not send a complete manuscript and there are missing pages, these will be noted. Also, if unauthorized copyright material had to be removed, a note will indicate the deletion.

**UMI**<sup>®</sup>

---

UMI Microform 1452259

Copyright 2008 by ProQuest LLC.

All rights reserved. This microform edition is protected against unauthorized copying under Title 17, United States Code.

ProQuest LLC  
789 E. Eisenhower Parkway  
PO Box 1346  
Ann Arbor, MI 48106-1346



# Thesis Approval

The Graduate College  
University of Nevada, Las Vegas

November 9, 2007

The Thesis prepared by

Ryan D. LeCounte

Entitled

Thermal Hydraulic Analysis of the High-Power RACE Target

is approved in partial fulfillment of the requirements for the degree of

Master of Science in Materials and Nuclear Engineering

Examination Committee Chair

Dean of the Graduate College

Examination Committee Member

Examination Committee Member

Graduate College Faculty Representative

## ABSTRACT

### **Thermal Hydraulic Analysis of The High-Power Race Target**

by

Ryan D. LeCounte

Dr. Daniel Cook, Examination Committee Chair  
Professor of Mechanical Engineering  
University of Nevada, Las Vegas

The High-Power RACE (HP-RACE) Target, a component of the Reactor-Accelerator Coupling Experiments (RACE), was designed to be coupled with a high-power electron linear accelerator (linac). The target was designed to be bombarded with electrons to produce photoneutrons via bremsstrahlung. This process will deposit 20 kW of beam power across a small mass of heavy metal and requires an analysis of the target's thermal system to ensure a safe design. In this study, the thermal hydraulics of the HP-RACE electron accelerator target is analyzed.

Low-power testing was performed at Idaho State University-Idaho Accelerator Center (ISU-IAC) using a linac capable of 1 kW, which is about one-twentieth of the designed operating power level. Calculations predicted conservative estimates of temperatures throughout the coolant channels and tungsten disks when compared to the low-power experimental data.

Fluent, a computational fluid dynamics code, was also utilized as an analysis tool for heat transfer as well as fluid flow. Temperature data from Fluent models was also conservative but more accurate than calculations, ~19% conservative versus ~34%. The fluid flow data predicted by Fluent also agreed with calculated and experimental values verifying the mathematical model and assumptions made in its development. This data also identified eddies in the outlet coolant channel at higher flow rates which could become problem areas in the target geometry and requires further study before the application of full power.

## TABLE OF CONTENTS

ABSTRACT .....	iii
LIST OF FIGURES .....	vi
ACKNOWLEDGMENTS .....	vii
CHAPTER 1 INTRODUCTION .....	1
Problem .....	2
Scope.....	2
CHAPTER 2 REVIEW OF RELATED LITERATURE.....	4
RACE Project.....	4
Argonne National Laboratories Work .....	7
CHAPTER 3 METHODOLOGY .....	10
Mathematical Approach .....	10
Experiment.....	14
Computational Estimates at 640 W.....	17
Computational Estimates at 20 kW .....	23
Fluent® Modeling.....	27
CHAPTER 4 FINDINGS OF THE STUDY .....	29
Analysis of Data .....	29
CHAPTER 5 SUMMARY, CONCLUSIONS, AND RECOMMENDATIONS .....	42
Discussion of Results.....	42
Conclusions and Recommendations for Further Study.....	43
APPENDIX I DATA .....	45
Data Recorded During the First 30 Seconds of the 640 W Experiment .....	45
Fluent Inputs .....	46
BIBLIOGRAPHY .....	48
VITA .....	49

## LIST OF FIGURES

Figure 2.1	The first RACE target with flange attached to the Cu-W target .....	5
Figure 2.2	The original RACE target modified with coolant lines.....	6
Figure 2.3	Cross section view of the High-Power RACE target.....	7
Figure 2.4	Argonne National Laboratories tungsten target.....	8
Figure 2.5	Temperature contours in a tungsten disk .....	9
Figure 3.1	Non-insulated HP-RACE target in line .....	16
Figure 3.2	Insulated HP-RACE target in line .....	17
Figure 3.3	Four of the seven HP-RACE target's tungsten disks.....	19
Figure 3.4	Curve fit of known Nusselt numbers.....	26
Figure 3.5	Completed model of the HP-RACE Target's .....	28
Figure 4.1	Coolant Temperature vs Time for 640 W Power Level Test.....	30
Figure 4.2	Slice taken axially through the HP-RACE Target's.....	31
Figure 4.3	Temperature contours (K) on the front surface .....	32
Figure 4.4	Temperature contours (K) on the rear surface .....	33
Figure 4.5	Velocity vectors (m/s) on a plane taken axially .....	34
Figure 4.6	Contours of velocity magnitude (m/s).....	35
Figure 4.7	Velocity vectors (m/s) on a plane .....	36
Figure 4.8	Close up of velocity vectors (m/s) entering coolant channels.....	37
Figure 4.9	Velocity vectors (m/s).....	38
Figure 4.10	Closeup of velocity vectors (m/s) entering coolant channels.....	38
Figure 4.11	Closeup of velocity vectors (m/s) exiting coolant channels .....	39
Figure 4.12	Closeup of velocity vectors (m/s) exiting .....	39
Figure 4.13	Velocity vectors (m/s) on a plane .....	40
Figure 4.14	Slice taken axially through the HP-RACE Target's.....	41



## ACKNOWLEDGMENTS

The author would like to express his thanks to Dr. Denis Beller, Dr. Charlotta Sanders, Dr. Daniel Cook and Dr. Julie Stagers for their help with providing information, software knowledge, and editorial work in the production of this document. Thanks are also expressed to the technical staff of the National Supercomputing Center for Energy and the Environment (NSCEE) for maintaining access to the required software, the Idaho State University-Idaho Accelerator Center staff for access to their facilities and equipment, and for their knowledge and aid in experimental setup and performance.

## CHAPTER 1

### INTRODUCTION

Transmutation is the process of converting one element into another by irradiating or bombarding it with radioactive particles. An example of this process is the transmutation of technetium-99, which has a half-life of hundreds of thousands of years. The absorption of a neutron by technetium-99 forms technetium-100 which decays to stable ruthenium in minutes [8]. Transmutation can be incorporated into the used nuclear fuel recycling process to reduce the radiotoxicity of the long lived isotopes and minor actinides that build up in fuel during its use.

The Reactor-Accelerator Coupling Experiments (RACE) are a set of Accelerator-Driven Subcritical System (ADSS) experiments that were meant to develop experimental data in support of transmutation [3]. The High-Power RACE (HP-RACE) target was the third iteration of the RACE target designed to accept the application of a 20 kW electron beam for bremsstrahlung photoneutron production. The thermal system of the target requires a thorough analysis to estimate its operational abilities and limitations.

## Problem

The HP-RACE target was designed and constructed as part of an undergraduate mechanical engineering design project. The project was focused on the design and fabrication of a cooled neutron producing electron target capable of accepting a 20 kW beam of ~25 MeV electrons, a 10-20x increase in the amount of power that previous RACE targets were capable of accepting. The increase in beam power was intended to increase the neutron production to a level greater than previous targets were capable of achieving [1]. The purpose of this study is to analyze the thermal system of the HP-RACE target to determine its ability to cool the target under the application of a 20 kW electron beam.

## Scope

This analysis is limited by the facilities, materials that the HP-RACE target was constructed of, and the computational fluid dynamics code available when this analysis began. The experimental setup and process was performed and controlled by Idaho State University's Idaho Accelerator Center (ISU-IAC). The electron linear accelerator that was available for testing was capable of producing the correct energy range of electrons, ~25 MeV, but produced a beam power of only 1 kW limiting testing to beam powers below this power. The only fluid made available was water and is therefore the only fluid considered as a coolant in this analysis. The measurements of coolant temperatures and flow were also limited to the two thermocouples and one volumetric flow meter provided by ISU-IAC. The use of materials in the target's construction, other than

what it was constructed of when this analysis began, is not considered.

Computer modeling of the HP-RACE was limited to Fluent [4], as it was the only computational fluid dynamics code available when this analysis began.

## CHAPTER 2

### REVIEW OF RELATED LITERATURE

#### RACE Project

The Reactor Accelerator Coupling Experiments (RACE) Project was formed as a multi-university Accelerator-Driven Subcritical System (ADSS) research project in support of transmutation of spent nuclear fuel [3]. It was started under the Department of Energy's Advanced Fuel Cycle Initiative (AFCI) to examine the coupling of accelerator-driven neutron sources and subcritical nuclear transmutation system. Photoneutrons were produced in these experiments using an electron accelerator and a heavy-metal target. Those neutrons were then used to induce fissions in subcritical systems [3].

The first RACE target consisted of a solid piece of heavy metal. Tungsten (75% tungsten and 25% copper mixture) was the material chosen to produce the desired ( $\gamma, n$ ) reactions. A stainless steel flange, welded to the solid tungsten target, connected the target to the end of an electron accelerator beam tube. The target was submerged in a 70 gallon tank of water which provided the necessary cooling, by natural convection, to dissipate the ~1 kW of beam power applied to the target (Fig. 2.1). The target was successfully tested at Idaho State University's Idaho Accelerator Center (ISU-IAC) [3].

The second phase of the RACE experiments focused on coupling the target with a TRIGA reactor. The coupling of the two required that the target no longer be submerged in a tank of water. The original target was modified by drilling coolant lines through the target body and cooling it using forced convection methods (Fig. 2.2). The target was successfully tested at 1.6 kW while coupled to a TRIGA reactor at the University of Texas at Austin [3].

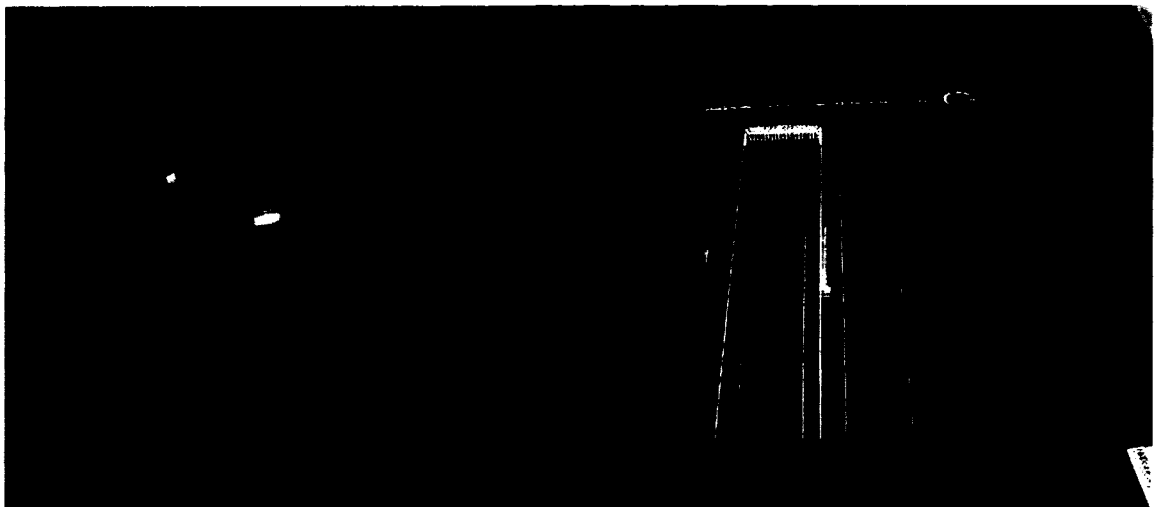


Figure 2.1 The first RACE target with flange attached to the Cu-W target (left). The first RACE target connected to an electron accelerator beam tube and inserted into its water tank. Graphite reflectors and fuel trays surround the target to check the fit prior to testing (right).

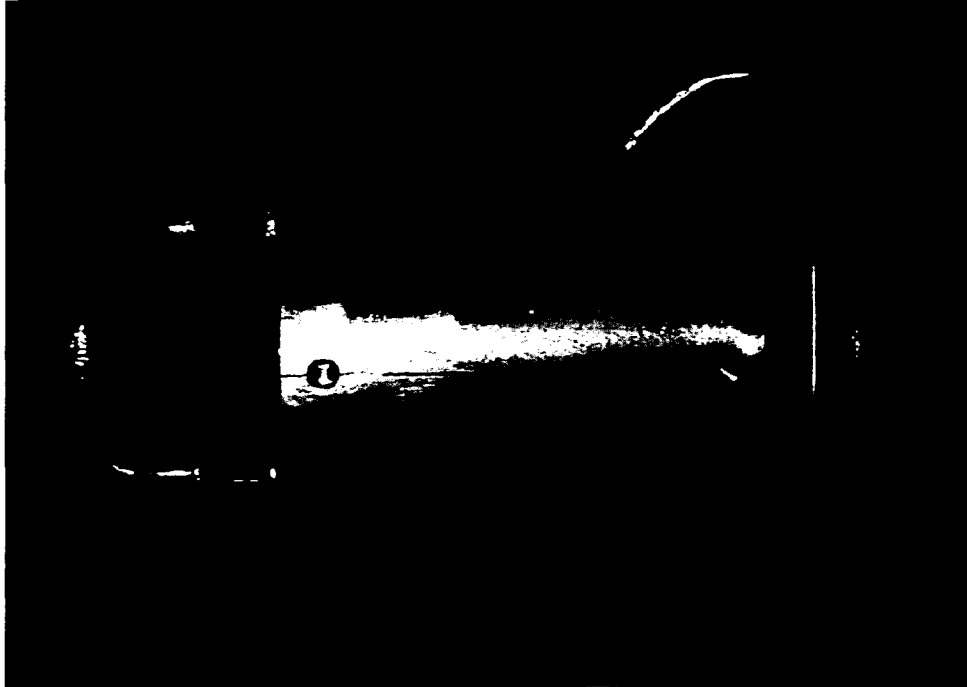


Figure 2.2 The original RACE target modified with coolant lines in preparation for coupling with the TRIGA reactor at University of Texas at Austin.

After the first successful coupling of a reactor and an accelerator-driven sub-critical system, a third iteration of the RACE target was designed to accept a much greater beam power to increase neutron production. In order to accept the planned 20 kW of beam power, the HP-RACE target was designed and fabricated from the ground up [10].

The first two RACE targets both used a solid piece of heavy metal for photon creation. The HP-RACE target material consists of seven thin tungsten disks, the same tungsten-copper mixture used in previous RACE targets, separated by aluminum spacers that form coolant channels between the disks. The stack of disks and spacers are housed in an aluminum body [10].

Unlike previous RACE targets, the HP-RACE target uses the tungsten for photon creation and a separate material for photoneutrons. Photons created in

the tungsten disks continue through the target's aluminum body to another cavity that contains a natural uranium fuel rod, responsible for the desired gamma and neutron reactions (Fig. 2.3) [10].

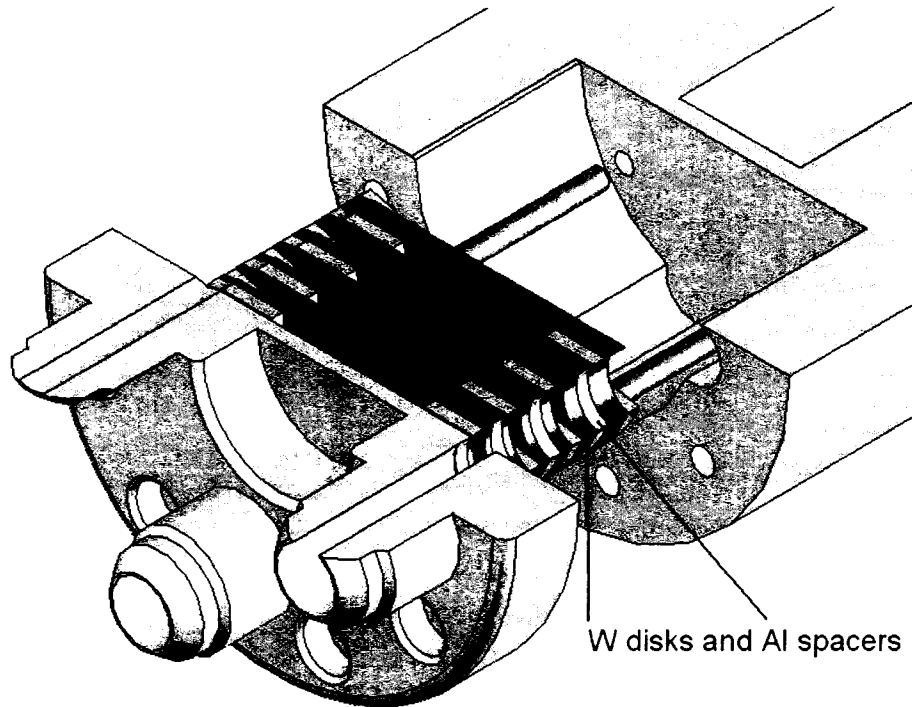


Figure 2.3 Cross section view of the High-Power RACE target disk stack, front cover, and body. The channel toward the top right of the figure is meant to house the uranium fuel rod.

#### Argonne National Laboratories Work

Argonne National Laboratories (ANL) has also performed design and analysis work of neutron producing electron targets. This target was designed to accept beam powers of up to 100 kW with electron energies of 100 to 200 MeV [9]. The target materials considered in the ANL work were uranium and tungsten [9]. The target design uses eight disks of the desired target material with channels between them for cooling much like the HP-RACE target (Fig. 2.4). The total



thickness of the target material was ~7 cm, over three times the amount used in the HP-RACE target. The larger amount of target material is due to the greater electron energies.

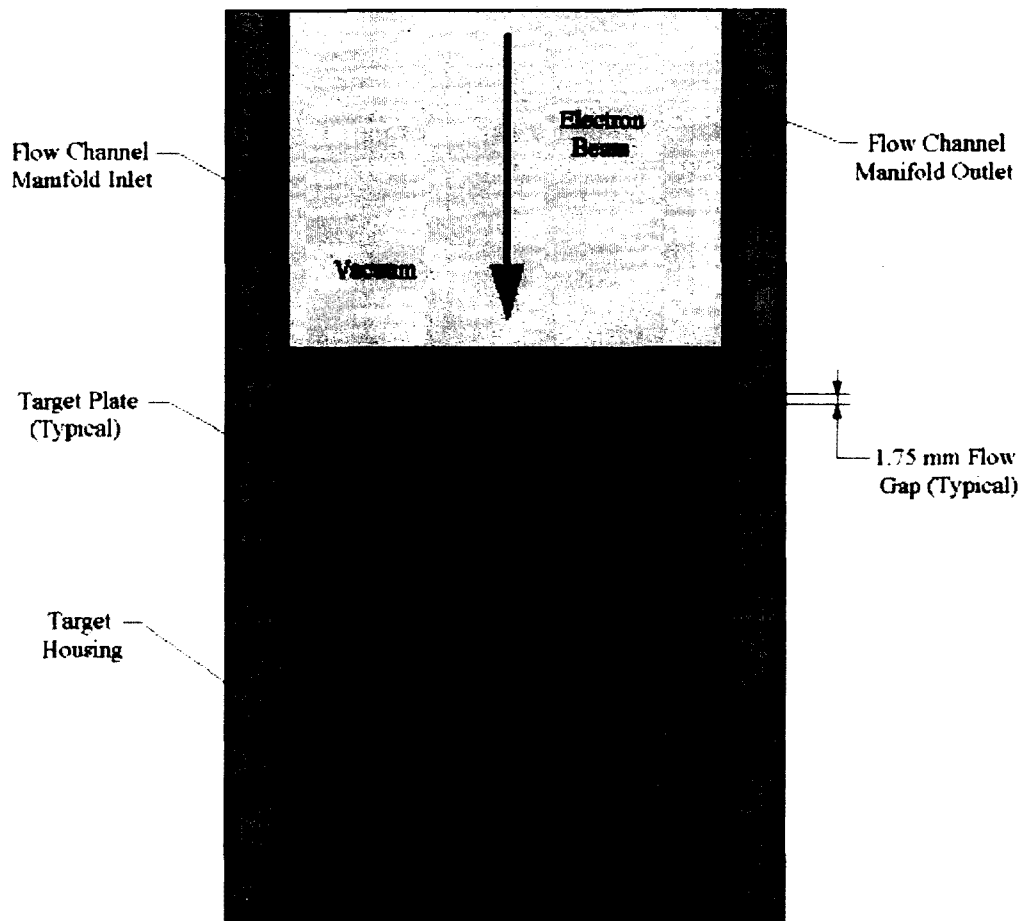


Figure 2.4 Argonne National Laboratories tungsten target configuration.

The ANL target uses two supply lines and two return lines to provide coolant to and from the disks. Both supply lines flow into each channel between the disks. The thermal hydraulic analysis revealed the greatest temperature in the

target disks to be created at the edges of the disk (Fig 2.5) where stagnant zones occurred in the coolant flow.

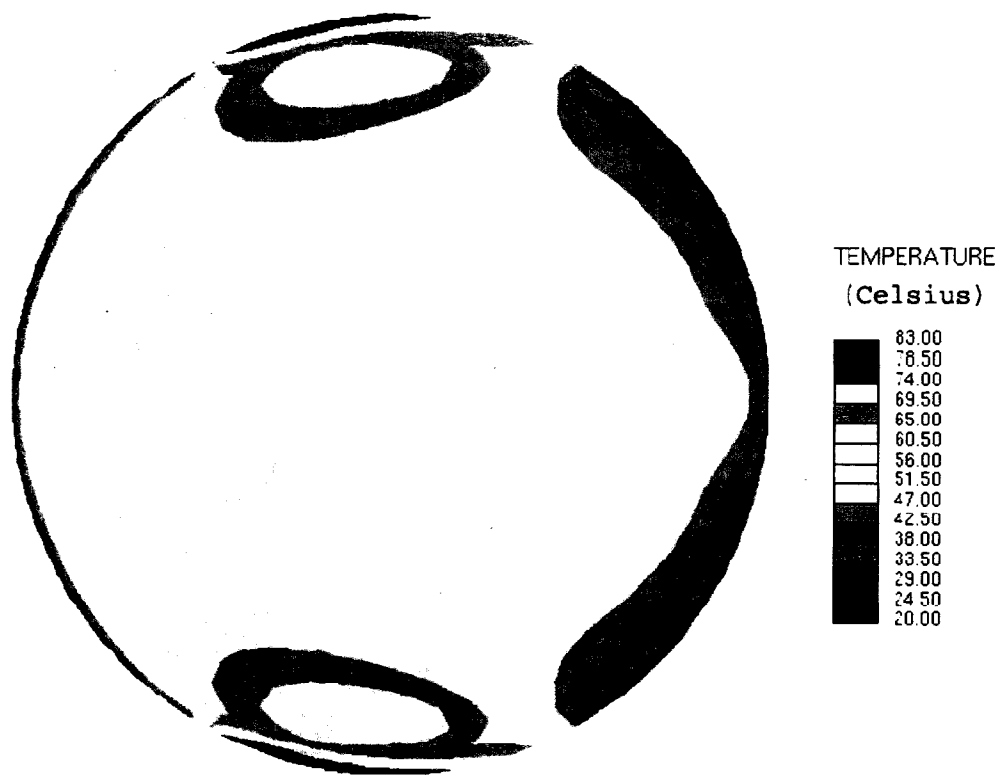


Figure 2.5 Temperature contours in a tungsten disk of the ANL target.

## CHAPTER 3

### METHODOLOGY

#### Mathematical Approach

Computational estimates were performed using general equations found in Incropera & Dewitt [6] and Moran & Shapiro [7]. A conservative approach was taken in choosing equations to represent the existing conditions of the HP-RACE target, at least to a first degree approximation.

The mathematical model began by determining the mean coolant temperature change from the inlet to the outlet. This was obtained from the total convective heat transfer to the coolant through all of the coolant channels, represented by

$$q_{conv} = \dot{m} c_p (T_{m,o} - T_{m,i}) \quad (3.1)$$

where  $q_{conv}$  is the power (kW),  $\dot{m}$  is the mass flow rate (kg/s),  $c_p$  is the specific heat (kJ/kg-K),  $T_{m,o}$  is the mean outlet coolant temperature, and  $T_{m,i}$  is the mean inlet coolant temperature (K). Equation 3.1 is formed from an overall energy balance and applies to internal flow regardless of the thermal conditions of the tube surface or the type of flow in the tube [6]. Equation 3.1 is solved for the mean change in coolant temperature ( $T_{m,o} - T_{m,i}$ ), to produce Equation 3.2.

$$T_{m,o} - T_{m,i} = \frac{\dot{q}_{conv}}{m c_p} \quad (3.2)$$

The temperature of concern, however, is the surface temperature of the tungsten disks. Since power is deposited in the tungsten disks, they will reach some steady-state temperature that is greater than the temperature of the coolant. The interface of the two has a temperature limitation that is defined by the boiling point of the coolant. This is due to the reduction in the cooling capabilities when a liquid changes states to a gas.

To estimate the surface temperature of the disks, Newton's law of cooling was used and is of the form

$$q'' = h(T_s - T_m) \quad (3.3)$$

where  $q''$  is the surface flux ( $W/m^2$ ),  $h$  is the convection coefficient ( $W/m^2-K$ ),  $T_m$  is the mean radial coolant temperature, and  $T_s$  is the surface temperature of the coolant channel. Solving Equation 3.3 for the change in temperature,  $T_s - T_m$ , yields

$$T_s - T_m = \frac{q''}{h} \quad (3.4)$$

The surface heat flux,  $q''$ , in Equation 3.4 was assumed to be a constant value which would be achieved during steady-state operation. The convection

coefficient of the coolant,  $h$ , is then the only quantity in Equation 3.4 that must be evaluated.

Determination of the convection coefficient varies depending on the nature of the flow in the coolant channel. It was assumed that the coolant was an incompressible fluid, water in its liquid state. It was also assumed that the flow through the channel for both turbulent and laminar flows was fully developed. The Reynolds number was used to determine the last required parameter, laminar or turbulent flow conditions.

For noncircular tubes, the Reynolds number is defined as

$$\text{Re}_{D_h} = \frac{\rho u_m D_h}{\mu} \quad (3.5)$$

where  $\rho$  is the density of coolant ( $\text{kg/m}^3$ ),  $u_m$  is the mean coolant velocity ( $\text{m/s}$ ),  $D_h$  is the hydraulic diameter ( $\text{m}$ ), and  $\mu$  is the viscosity of the coolant ( $\text{N}\cdot\text{s/m}^2$ ) [6]. Since the channels between the disks are not circular, the diameter in this equation is an effective diameter and is a function of the cross sectional area ( $A_c$ ) and the wetted perimeter ( $P$ ) [6]. It is defined as

$$D_h = \frac{4A_c}{P} \quad (3.6)$$

The mean coolant velocity needed in Equation 3.6 is the velocity of the coolant through a coolant channel. Considering a known volumetric flow rate at an

individual inlet supplying four of the eight channels which all have equal cross sections and assuming the incoming coolant is equally divided between the four coolant channels, then the relationship between the supply line and coolant channel flow rates can be represented by

$$\frac{A_1 V_1}{\nu_1} = 4 \frac{A_2 V_2}{\nu_2} \quad (3.7)$$

where  $A_1 V_1$  is the volumetric flow rate in either one of the two supply lines ( $\text{m}^3/\text{s}$ ),  $A_2 V_2$  is the volumetric flow rate in any one of the coolant channels at the desired location ( $\text{m}^3/\text{s}$ ), and  $\nu_1$  and  $\nu_2$  are the specific volumes ( $\text{m}^3/\text{kg}$ ) of the coolant at their respective temperatures [7]. For small changes in temperature,  $\nu_1/\nu_2 \approx 1$ .

The mean velocity in any channel is then

$$u_m = V_2 = \frac{A_1 V_1}{4 A_2} \quad (3.8)$$

The convection coefficient was determined from the expression

$$h = Nu_D \frac{k}{D_h} \quad (3.9)$$

where  $k$  is the thermal conductivity of the coolant ( $\text{W}/\text{m}\cdot\text{K}$ ),  $D_h$  is the hydraulic diameter (m), and  $Nu_D$  is the Nusselt number [6]. The Nusselt number for

turbulent flow conditions in the HP-RACE was determined from Gnielinski's modified Nusselt number calculation which is considered to be an accurate computation with errors of less than 10% compared to errors in the range of 25% using unmodified Nusselt number calculations. The expression is

$$Nu_D = \frac{(f/8)(Re_{D_h} - 1000)Pr}{1 + 12.7(f/8)^{1/2}(Pr^{2/3} - 1)} \quad (3.10)$$

where Pr is the Prandtl number, determined from tables, and  $f$  is the friction factor calculated using

$$f = (0.790 \ln(Re_{D_h}) - 1.64)^{-2} \quad (3.11)$$

The above calculation of  $f$  is valid for turbulent flow and smooth inner tube surfaces [6]. Equation 3.10 is valid for smooth inner tube surfaces,  $0.5 < Pr < 2000$ , and  $3000 < Re_{D_h} < 5 \times 10^6$  [6].

For laminar flow conditions in the HP-RACE target, the Nusselt number was obtained from Incopera and DeWitt, Table 8.1 [6]. Equation 3.9 was then used to determine the convection coefficient.

### Experiment

The HP-RACE target's cooling system was designed with the coolant supply and return lines attached to the face of the target that also accepts the electron

beam. This design would not allow the target to be directly attached to the electron accelerator beam tube. Instead, the beam tube was capped using a 0.001 inch thick piece of stainless steel, known as a beam tube window, clamped between two flanges. The target was placed a few inches away from the end of the beam tube for clearance of the coolant lines. The front end of the target, containing the tungsten disks, was placed facing the end of the beam tube with the axis of the beam tube and the axis of the target aligned. Polyethelene blocks and aluminum spacers were used for height adjustment when aligning the target and beam tube (Fig. 3.1).

The target was designed to accept a uranium fuel rod to produce the necessary ( $\gamma$ , n) reactions, but at the time of testing this option was not available. The cavity in the rear of the target was filled with lead pellets in place of the uranium fuel rod to produce photo-neutrons.

Two testing sessions were performed with the HP-RACE target coupled to a linac at ISU-IAC. The first session consisted of two power levels, 389 W and 583 W. The second session was more intensive including power levels of 100 W through 500 W in 100 W increments and a final 640 W test.

During the first testing session the target was placed in direct contact with the polyethylene blocks and aluminum spacers for alignment with the accelerator (Fig. 3.1). Thermocouples were connected to the inlet and outlet lines to monitor coolant temperatures and a volumetric flow meter was connected to a main coolant supply line that supplied both of the target's coolant inlets to monitor the



coolant flow rate. A third thermocouple was placed on the outer surface of the target to monitor the target's body temperature.

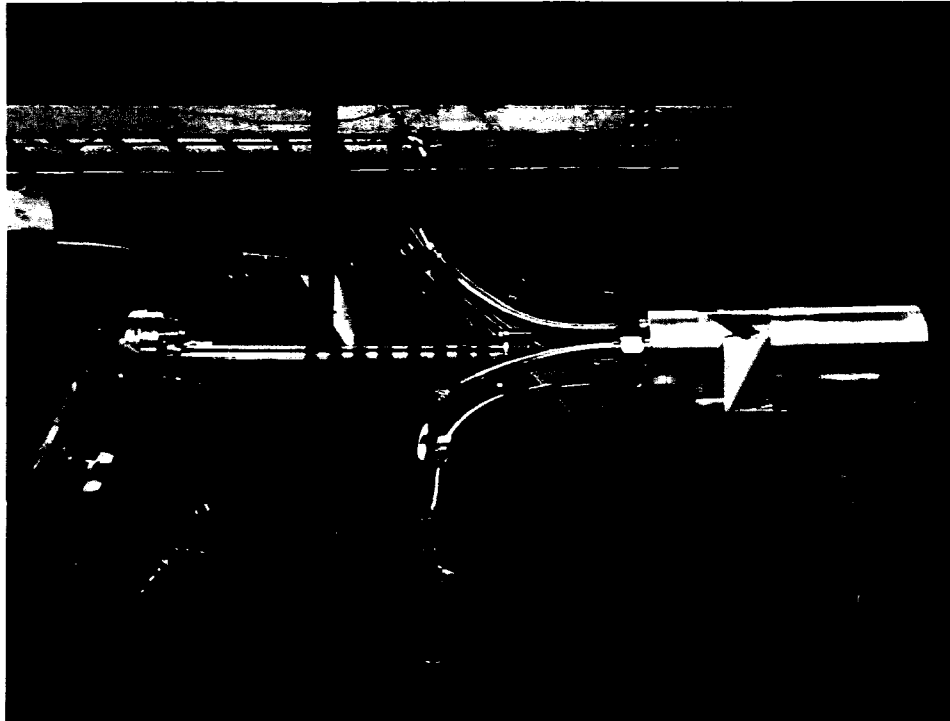


Figure 3.1 Non-insulated HP-RACE target in line with the electron accelerator and coolant lines connected.

The second session of testing was setup in the same manner as the first with a couple of changes in addition to the wider range of power levels. During this session the outer surface of the target was insulated to reduce conduction to the spacers and convection from the outer surface (Fig. 3.2). This was done to force as much of the deposited power as possible to be removed by the coolant. The target was then placed on top of the polyethylene blocks and aluminum spacers for alignment with the accelerator. Thermocouples were connected to the inlet and outlet lines to monitor coolant temperatures and a volumetric flow meter was connected to a main coolant supply line that supplied both of the target's coolant

inlets to monitor the coolant flow rate. A third thermocouple was not available at the time of testing so no means of measuring the target's body temperature was possible. The first 30 seconds of data acquired are recorded in Appendix I.

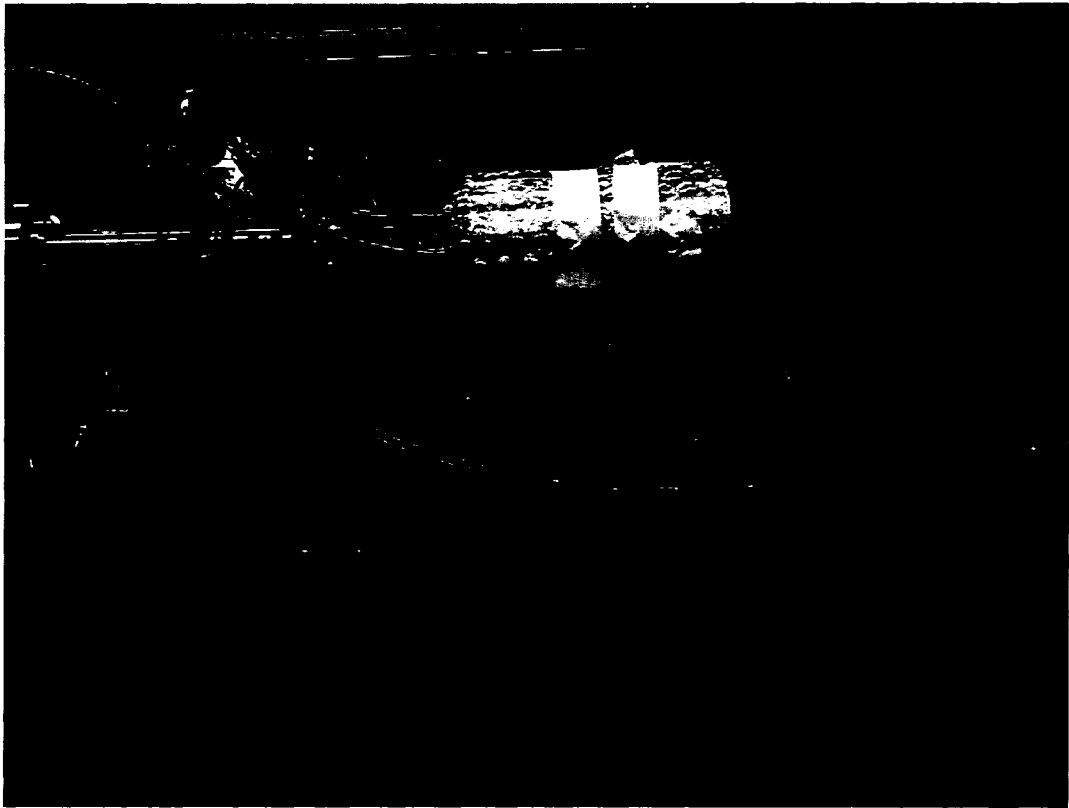


Figure 3.2 Insulated HP-RACE target in line with the electron accelerator with coolant lines attached.

### Computational Estimates at 640 W

Temperature estimates were calculated for the 640 W experiment since the insulated surface was a more accurate representation of the adiabatic outside surface assumption made in the mathematical theory development. Table 3.1 lists the values for various properties of water used in the calculations. The properties of water were taken from Incopera and DeWitt, Table A.6 [6], at the

expected outlet coolant temperature of 305 K, ~7 K over room temperature (~293 K).

Table 3.1 Properties of Water <sup>a</sup>

Specific Volume $v$ (m <sup>3</sup> /kg)	Density <sup>b</sup> $\rho$ (kg/m <sup>3</sup> )	Specific Heat $c_p$ (kJ/kg-K)	Viscosity $\mu$ (N-s/m <sup>2</sup> )	Thermal Conductivity $k$ (W/m-K)	Prandtl Number Pr
1.01E-03	9.95E+02	4.18E+00	7.69E-04	6.20E-01	5.20E+00

Notes:

a - Values obtained from Incopera and DeWitt, Table A.6 for water at 305 K

b - Calculated,  $\rho=1/v$

The change in coolant temperature for the 640 W experiment was estimated using Equation 3.2 and a main supply line volumetric flow rate of 1.07 L/min converted to  $1.78 \times 10^{-5} \text{ m}^3/\text{s}$ .  $T_{m,o} - T_{m,i}$  was found to be

$$T_{m,o} - T_{m,i} = \frac{0.640 \text{ kW}}{(1.78 \times 10^{-5} \text{ m}^3 / \text{s})(995 \text{ kg} / \text{m}^3)(4.18 \text{ kJ} / \text{kg} \cdot \text{K})} = 8.7 \text{ K}$$

This value assumes that all of the power is deposited in the tungsten disks and carried away by the coolant alone. This is a conservative assumption, in that it will predict greater temperature changes, and is discussed in chapter 4.

Evaluation of the change in the surface temperature of the disks began with the velocity of the coolant in an individual channel. The channel velocity was calculated using the cross sectional area of a channel at its widest point, the inlet

volumetric flow rate ( $A_1V_1$ ), and Equation 3.8. Determining the channel velocity at its widest cross section (Fig. 3.3) results in the lowest average velocity in the channel which reduces the Reynolds number calculation to a minimum. This will allow for the lowest convection coefficient and a larger coolant temperature change estimate building conservatism into the results. Channel dimensions, channel cross sectional area, and coolant supply line volumetric flow rate are tabulated in Table 3.2 along with the calculated average channel velocity at the channel's widest point.

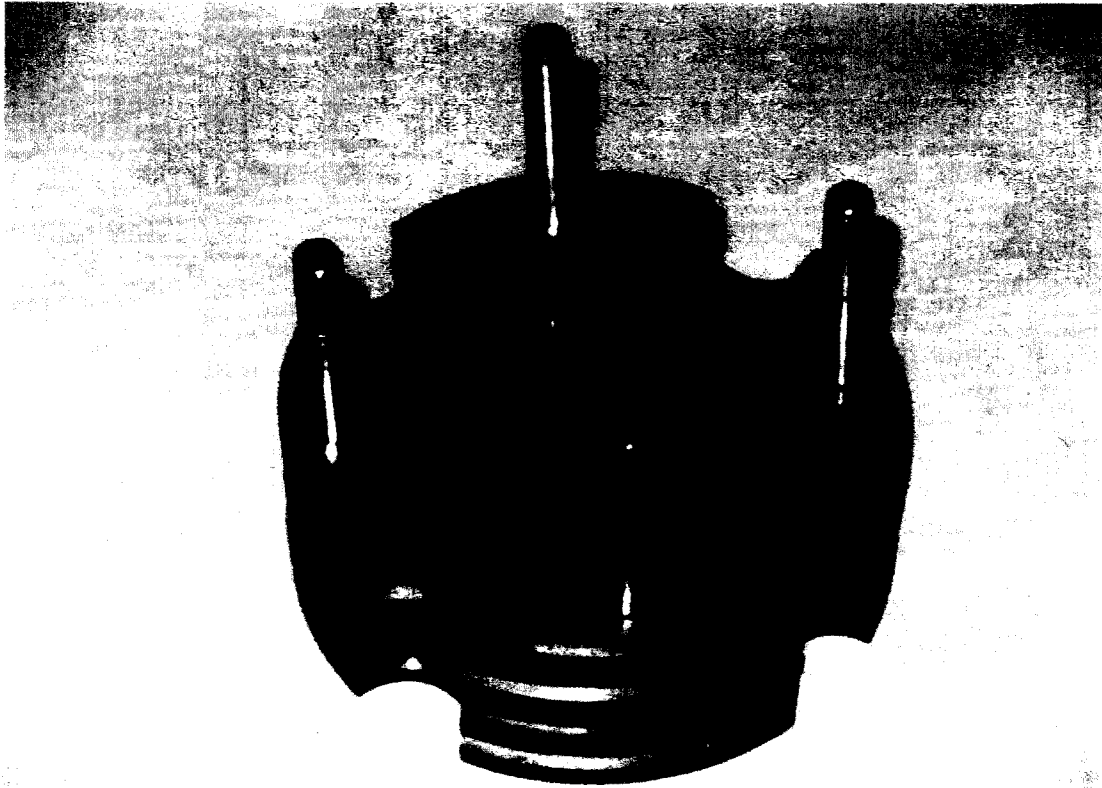


Figure 3.3 Four of the seven HP-RACE target's tungsten disks assembled with aluminum spacers and steel alignment pins. The uppermost disk and spacers show the shape of each coolant channel. Also, the increase in disk thickness can be seen for the first four disks.

Table 3.2 Coolant Channel Velocity for 640 W Power Input

Volumetric Flow Rate in Each Supply Line (Main Line/2) $A_1V_1$		Channel Depth $a$	Widest Channel Width $b$	Largest Channel Cross-Sectional Area $A_2$	Lowest Average Velocity of Coolant in Channel $u_m$
(L/min) <sup>a</sup>	(m <sup>3</sup> /s) <sup>b</sup>	(m) <sup>a</sup>	(m) <sup>a</sup>	(m <sup>2</sup> ) <sup>c</sup>	(m/s) <sup>c</sup>
5.34E-01	8.90E-06	2.50E-03	3.00E-02	7.50E-05	2.97E-02

Notes:

a - Measured quantities

b - Conversion factor of  $1.667 \times 10^{-5}$  (m<sup>3</sup>/s) / 1 (L/min) applied

c - Calculated values

The total power ( $P_t$ ) applied to the target is assumed to be evenly divided amongst the seven tungsten disks. The power applied to each disk ( $P_d$ ) is then

$$P_d = \frac{P_t}{7} \quad (3.13)$$

or

$$P_d = \frac{640}{7} = 91.4W$$

Evaluation of  $q''$  to be removed by each channel was determined by dividing the power deposited ( $P_d$ ) in each disk by the cooling area of each channel ( $A_{cd}$ ).

$$q'' = \frac{P_d}{A_{cd}} \quad (3.14)$$

To maintain conservatism, the cooling area was calculated using the area that the electron beam was deposited over instead of the entire coolant channel and was estimated to be  $1.41 \times 10^{-3} \text{ m}^2$ , assuming the electron beam is deposited over a circular area with a radius of  $\sim 0.015 \text{ m}$ . Based on the assumption that the coolant is the only means of escape, the surface heat flux that the cooling system must remove from each disk for the 640 W case was found to be

$$q'' = \frac{91.4W}{0.00141m^2} = 6.47 \times 10^4 W / m^2$$

This surface flux assumes that all of the beam power is deposited in the tungsten disks.

The flow in the channels must be determined to be laminar or turbulent using Equations 3.5, .6, and .8. The hydraulic diameter was determined using Equation 3.6 and the channel dimensions recorded in Table 3.2. It was calculated to be

$$D_h = \frac{4 \cdot 0.0325 \cdot 0.0025}{2 \cdot (0.0325 + 0.0025)} = 0.0046m$$

The velocity in each coolant channel was calculated using Equation 3.8 and recorded in Table 3.2. Using these values, Equation 3.5, and the properties of water from Table 3.1 the Reynolds number was determined to be

$$\text{Re}_{D_h} = \frac{(995 \text{ kg/m}^3)(0.0297 \text{ m/s})(0.0046 \text{ m})}{0.000769 \text{ N} \cdot \text{s/m}^2} = 177$$

This indicates laminar flow since the onset of turbulent flow does not occur until a Reynold's number of approximately 2300 with fully developed turbulent flow having a Reynolds number of >10,000.

For internal fully developed laminar flow, the Nusselt number is obtained from Incopera and DeWitt, Table 8.1 [6]. The value of  $\text{Nu}_{D_h}$  is based on the ratio of the channel width to its depth,  $b/a$ . The HP-RACE target coolant channels have a ratio of 12 which falls between a ratio of 8 and  $\infty$  in the table. To obtain the value for a ratio of 12, the data from Table 8.1 for ratios of 1.43 through 8 were graphed and fit with a trendline (Fig 3.4). The equation of the trendline was used to extrapolate out to the desired ratio. The resulting Nusselt number was calculated to be 7.50. Using this value, the value for  $k$  recorded in Table 3.1, the calculated value of  $D_h$ , and Equation 3.9, the convection coefficient was found to be

$$h = 7.50 \frac{0.620 \text{ W/m} \cdot \text{K}}{0.0046 \text{ m}} = 1011 \text{ W/m}^2 \cdot \text{K}$$

Applying this value to Equation 3.4 to find the change in the surface temperature of the disk over that of the coolant results in

$$T_s - T_m = \frac{6.47 \times 10^4 \text{ W/m}^2}{1011 \text{ W/m}^2 \cdot \text{K}} 63.9 \text{ K}$$

This is an expected total change in the temperature of the disk surface of approximately 63.9 K + 8.7 K = 72.6 K assuming the disk and coolant temperatures are at equilibrium when power is applied to the target.

### Computational Estimates at 20 kW

The 20 kW beam power will require a greater convection coefficient to cool the target. This is achieved by increasing the volumetric flow rate of the coolant to increase the Reynold's number to >10,000, for fully developed turbulent flow. Beginning with a hypothesized total volumetric flow rate in the main line supplying both coolant lines of 24 gpm ( $1.514 \times 10^{-3} \text{ m}^3/\text{s}$ ), as estimated in the design of the HP-RACE target [10], the resultant change in coolant temperature between the inlet and outlet coolant lines was determined using Equation 3.2, the values from Table 3.1 and the applied power of 20 kW, and was found to be

$$T_{m,o} - T_{m,i} = \frac{20 \text{ kW}}{(1.514 \times 10^{-3} \text{ m}^3 / \text{s})(995 \text{ kg} / \text{m}^3)(4.18 \text{ kJ} / \text{kg} \cdot \text{K})} = 3.2 \text{ K}$$

This assumes that all of the beam power is deposited in the tungsten disks.

Using the cross sectional area of each channel calculated and recorded in Table 3.2, the volumetric flow rate in each supply line, 12 gpm ( $7.751 \times 10^{-4} \text{ m}^3/\text{s}$ ), and Equation 3.8 the velocity in any channel is found to be



$$u_m = \frac{7.571 \times 10^{-4} \text{ m}^3 / \text{ s}}{4 \cdot 7.50 \times 10^{-5} \text{ m}^2} = 2.52 \text{ m / s}$$

The Reynolds number is then

$$\text{Re}_{D_h} = \frac{(995 \text{ kg / m}^3)(2.52 \text{ m / s})(0.0046 \text{ m})}{0.000769 \text{ N} \cdot \text{ s / m}^2} = 15,201$$

This clearly indicates fully developed turbulent flow in the channels, a desired result since turbulent flow has a much greater convective coefficient allowing greater cooling capabilities. Calculating the friction factor from Equation 3.11 and using that result in Equation 3.10, Nusselt number calculation for turbulent flow, along with the Prandtl number recorded in Table 3.1 gives

$$f = (0.790 \ln(15021) - 1.64)^{-2} = 0.0287$$

and

$$\text{Nu}_D = \frac{(0.0287/8)(15021 - 1000)5.20}{1 + 12.7(0.0287/8)^{1/2}(5.20^{2/3} - 1)} = 103.7$$

The convection coefficient is then determined by Equation 3.9, the value for  $k$  recorded in Table 3.1 and the calculated value of  $D_h$ .

$$h = 103.7 \frac{0.620}{0.0046} = 13,975 W / m^2 \cdot K$$

The resulting estimate for the change in the disk surface temperature is determined by  $q''$  (Equations 3.13 -3.14), which is

$$q'' = \frac{20000W/7}{0.00141m^2} = 2.026 \times 10^6 W / m^2$$

and Equation 3.4,

$$T_s - T_m = \frac{2.026 \times 10^6 W / m^2}{13975 W / m^2 \cdot K} = 145 K$$

The total increase in the disk surface temperature is then  $145 K + 6.4 K = 151.4 K$  assuming all of the beam power is deposited in the tungsten disks.

**Nusselt Number versus Ratio of Channel Width (b) to Channel Depth (a)**

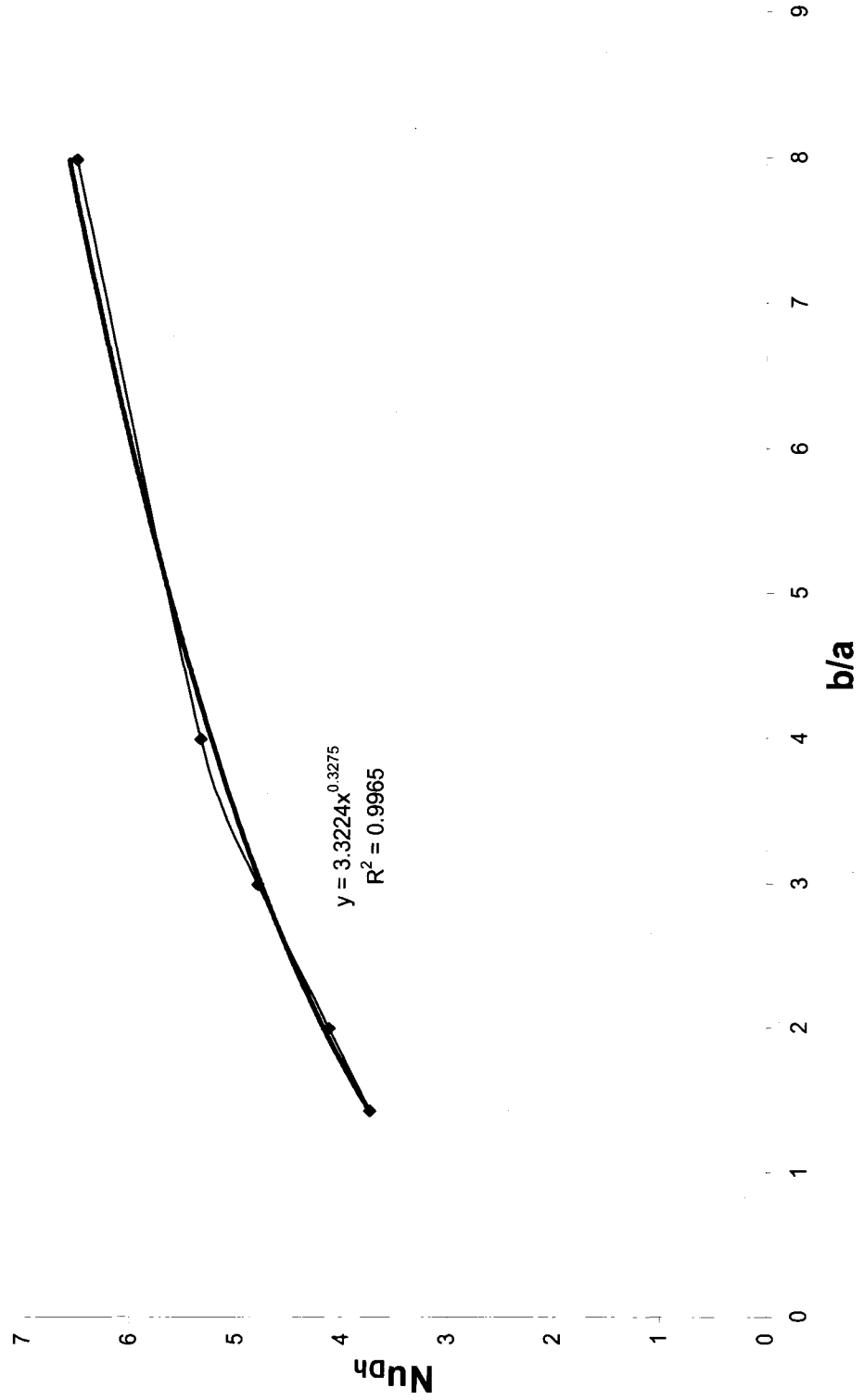


Figure 3.4 Curve fit of known Nusselt numbers for laminar flow in rectangular tubes.

## Fluent® Modeling

Fluent [4], a computational fluid dynamics code, was used to verify theoretical results and evaluate problem areas that may arise in the target. Gambit, a 3-D modeling software package included with Fluent, was used to create a 3-D model of the front portion of the target. Using the same assumptions used in the calculations allowed the model to consist of only the tungsten disk stack, spacers, and coolant (Fig. 3.5). Building the model in this manner allowed the results to be directly compared to calculated values and drastically reduced the required amount of computing power and time. A mesh, using a node spacing of 0.01 cm, was then laid across the model surface and throughout its volume. The node spacing was chosen by balancing the smaller node spacing requirements of the thin disks in the target geometry and the least amount of total nodes to reduce computing power requirements.

The mesh created using Gambit was then imported into Fluent. Materials were defined using a combination of materials available in the Fluent library and self defined materials (see Appendix). Fluid flow was achieved by defining a velocity inlet which is the velocity of the fluid in the inlet line. Power was applied to the model by defining a volume source in the center of each disk, in units of  $W/m^3$ , determined for each individual disk by the product of the surface flux and disk thickness. The source terms used are tabulated in the Appendix. Three dimensional double precision coupled, SIMPLE, and SIMPLEC models were all considered for both the low and high power scenarios.

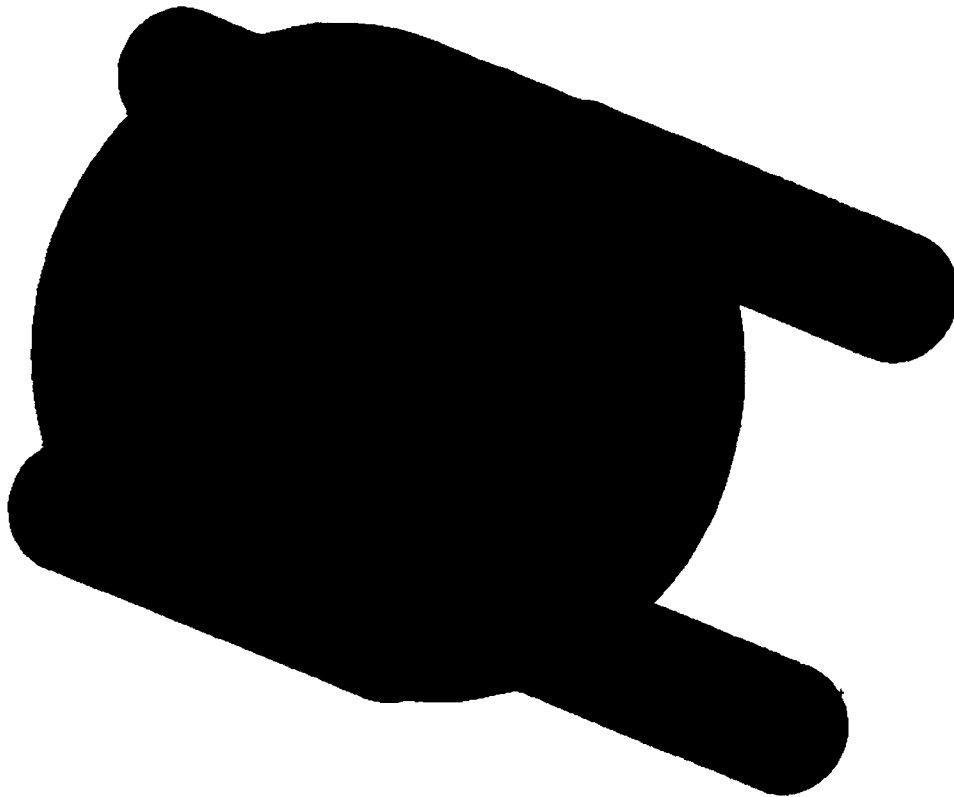


Figure 3.5 Completed model of the HP-RACE Target's assembled tungsten disk stack and coolant built and meshed in Gambit then imported into Fluent.

## CHAPTER 4

### FINDINGS OF THE STUDY

#### Analysis of Data

The 640 W experimental test yielded results lower than those calculated. Figure 4.1 displays inlet and outlet temperature data plotted for the 640 W test. The difference between the experimental inlet and outlet temperatures averaged approximately 5.7 °C during steady-state operation. In the first twenty seconds of the experiment, the coolant was run with no beam power applied to the target. This can be seen in the graph by the decrease in temperature for both the inlet and outlet. In this region the original data indicated a 1.3 °C bias between the thermocouples that was accounted for in the creation of Figure 4.1. The bias was calculated by averaging the difference in the inlet and outlet temperature data obtained before the beam was applied to the target.

Calculations using the mathematical model resulted in a temperature difference of approximately 8.7 °C between the coolant inlet and outlet when using a 640 W beam power. This temperature change was expected to be high because the mathematical model assumed ideal conditions. A disk surface temperature change of 72.6 °C was also predicted, which is less than the boiling point of the coolant. This value could not be verified since no means to retrieve data on the interior of the cooling system was available.

### Inlet & Outlet Coolant Temperatures (640 Watt Experiment, Corrected for Bias)

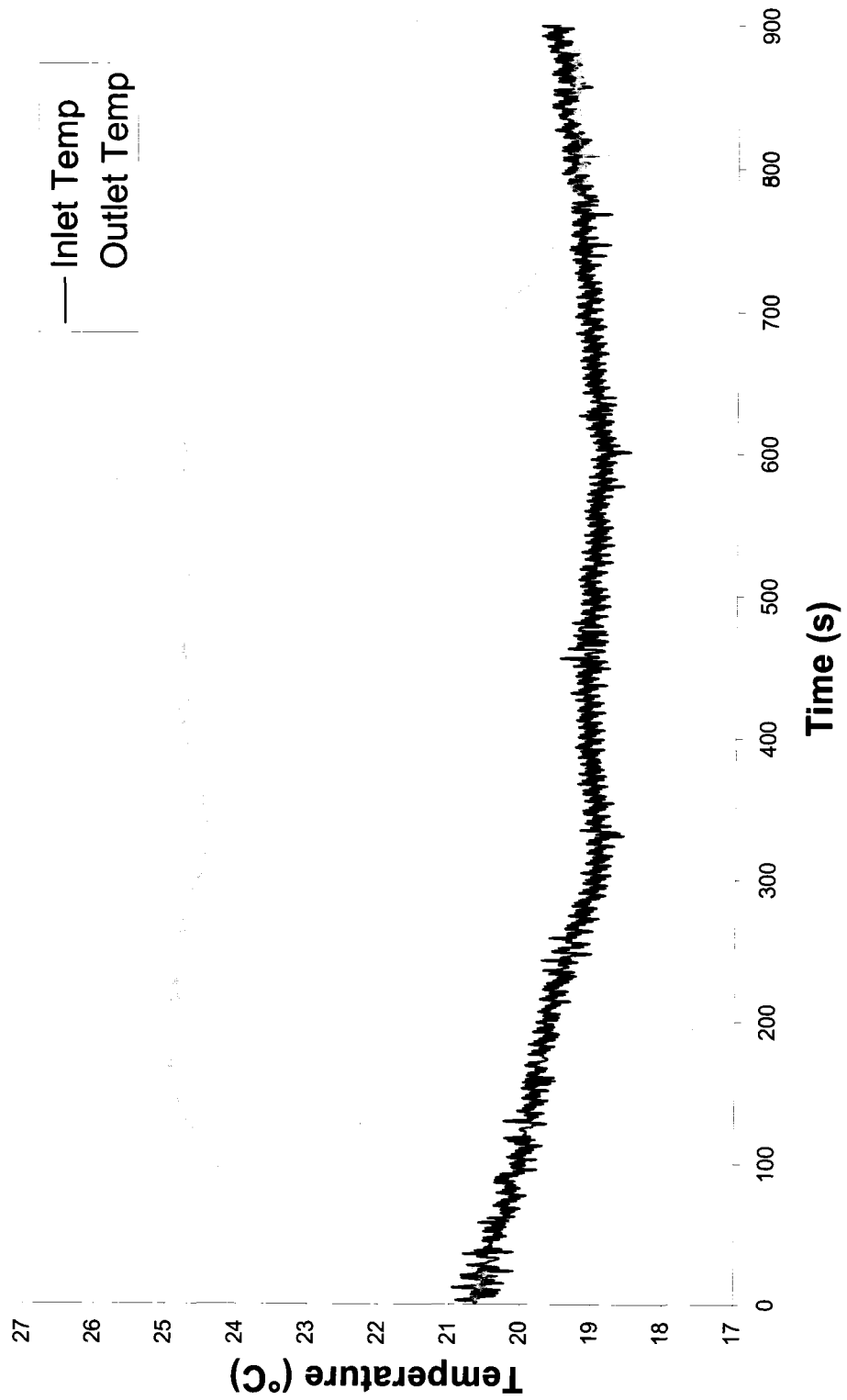


Figure 4.1 Coolant Temperature vs Time for 640 W Power Level Test

Fluent results revealed valuable information about the target performance. Figure 4.2 shows temperature contours on a slice taken along the axis of the target and through one of the main water inlets and outlets. The coolant inlet is the darker blue leg with temperatures of 300 K (27 °C). The lighter blue leg is the coolant outlet and has an average temperature of approximately 307 K (34 °C), resulting in an average temperature difference of 7 °C. This result is conservative when compared to the experimental results but not as conservative as the calculations which was the expected outcome.

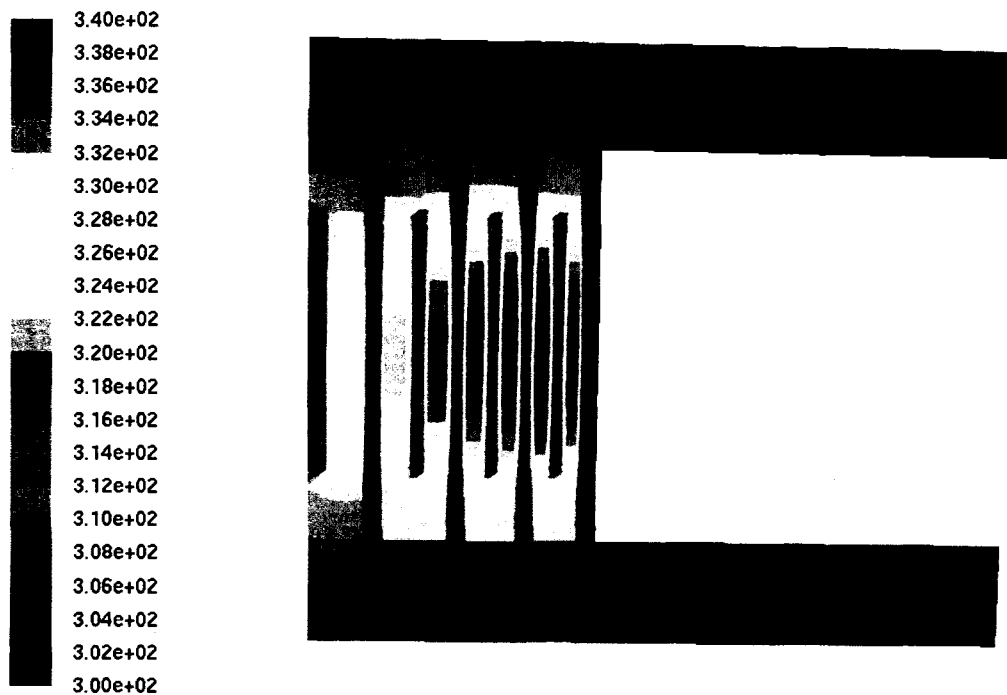


Figure 4.2 Slice taken axially through the HP-RACE Target's tungsten disk stack and cooling system showing temperature contours (K) at 640 Watts of beam power.

As mentioned previously, the inlet and outlet temperatures of the coolant give only an overview of the target's performance. The maximum amount of power



that can be applied to the target is limited by the boiling point of the coolant which will occur at the interface between the coolant and disk surface. Figures 4.3 and 4.4 are slices taken perpendicular to the axis of the target and show temperature contours on the front and rear surfaces of the second tungsten disk, the disk that appears to have the greatest temperature increase. Temperature increases range from 30 °C to a maximum of 39 °C. The maximum temperature increase is much lower than the mathematical models predicted, 72.6 °C. There is no experimental data to compare these results to due to the lack of means available to acquire temperatures on the interior of the cooling system.

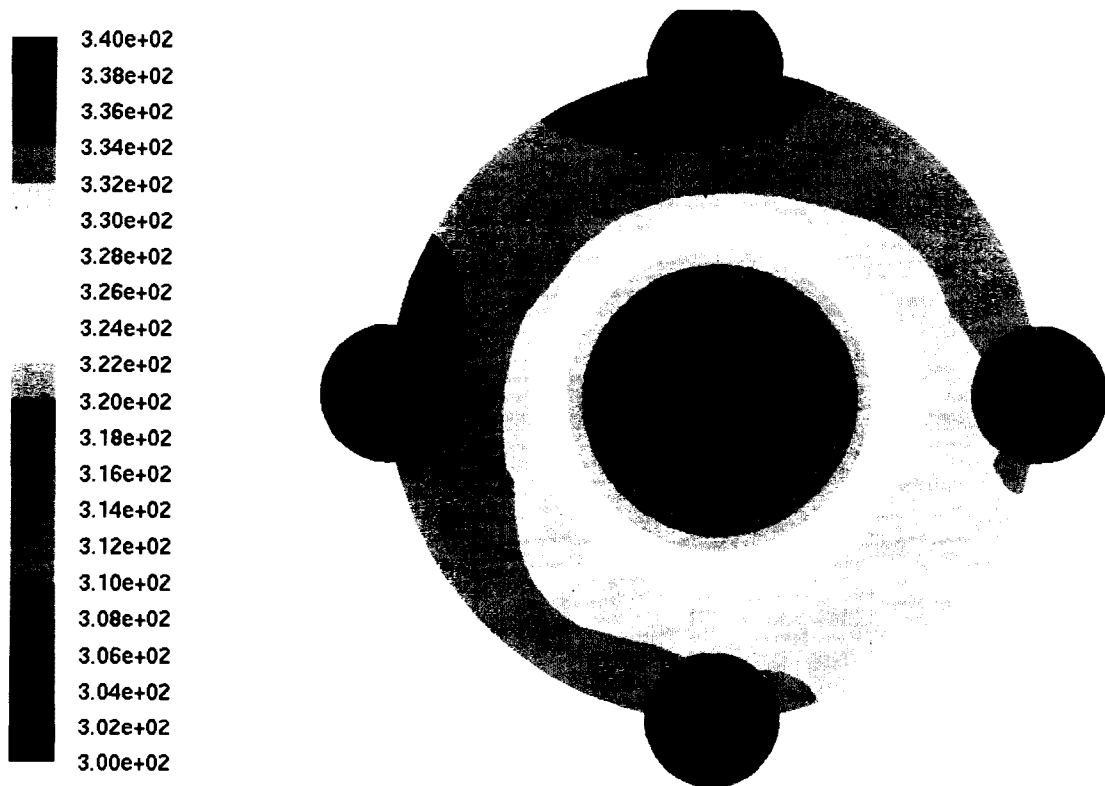


Figure 4.3 Temperature contours (K) on the front surface of the second tungsten disk of the HP-RACE Target with 640 W of beam power.

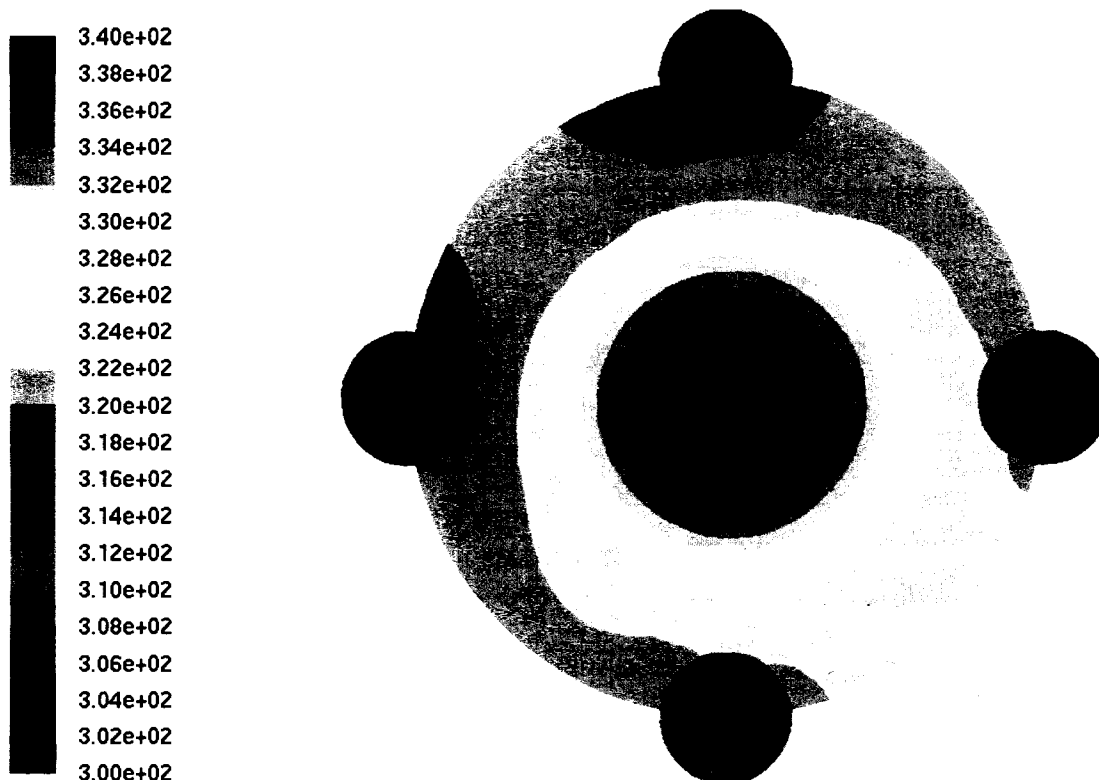


Figure 4.4 Temperature contours (K) on the rear surface of the second tungsten disk of the HP-RACE Target with 640 W of beam power.

An important part of the Fluent analysis was to predict flow conditions through the target's cooling system. Figures 4.5 through 4.8 show velocity contours and velocity vectors on slices taken through sections of the target's cooling system. Figure 4.5 displays velocity vectors through one of the main supply lines and the four coolant channels it supplies. It can be seen that as the flow of coolant enters each channel the velocity of the flow in the supply line is reduced. Of more importance is the equality of flow through each channel. This verifies the assumption made in the mathematical model that the incoming flow would be equally divided between the four channels due to their identical cross sections.

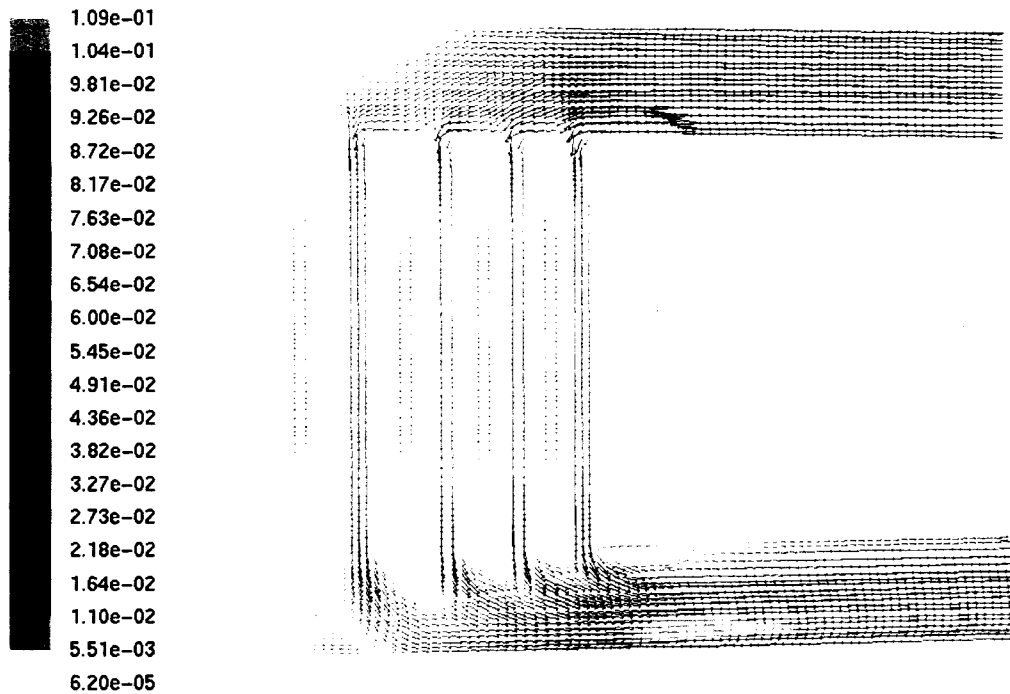


Figure 4.5 Velocity vectors (m/s) on a plane taken axially through the HP-RACE Target's tungsten disk stack and cooling system with an input volumetric flow rate of 0.535 L/min.

Figure 4.6 is a slice taken through the first coolant channel and shows contours of velocity magnitude. Through the center of the disk, where the coolant channel is at its widest, it can be seen that the velocity has the same average magnitude as the value that the mathematical model predicted, 0.0297 m/s. This figure also predicts slightly higher flow velocities toward the edges of the channel and slower velocities in the center. This is a great concern since this is the area where the beam deposits its power and where the coolant removes the bulk of the heat. A significantly slower flow across the center of any of the disks could cause a hot spot leading to boiling of the coolant and failure of the target material.

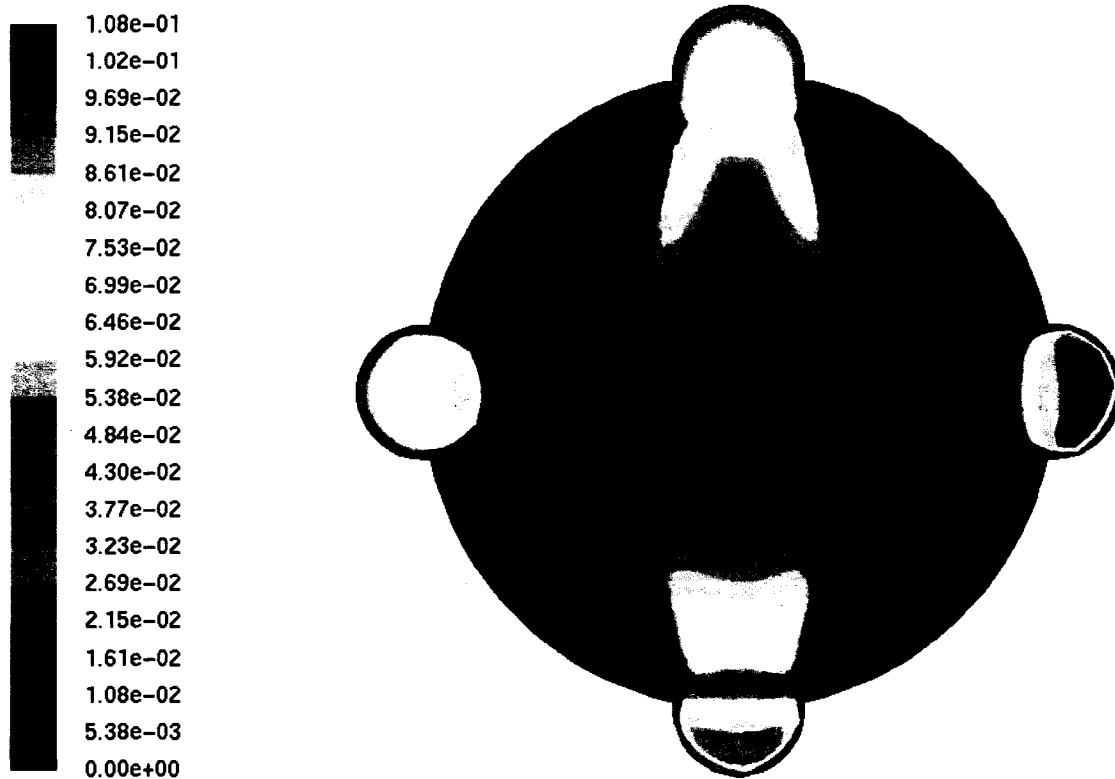


Figure 4.6 Contours of velocity magnitude (m/s) on a plane taken perpendicular to the HP-RACE Target's axis through a water channel with an input volumetric flow rate of 0.535 L/min.

Looking at the velocity vectors shown in Figure 4.7 it can be seen that the slower velocity at the center of the disk is not due to eddies formed in the cooling fluid. This is a good indication that this will not become a stagnant zone. This result may limit the target's capabilities depending on how much of a reduction in velocity magnitude there is at the center and may become more of a concern at higher flow rates.

A closeup view of the coolant entering each channel, Figure 4.8, shows no indication of eddies forming where the fluid makes a ninety degree turn from the supply line to the coolant channels. This was expected to be an area of concern

for stagnant zones because of the abrupt change in direction. Again, stagnant zones may become an issue in these areas at greater flow rates.



Figure 4.7 Velocity vectors (m/s) on a plane taken perpendicular to the HP-RACE Target's axis through a water channel with an input volumetric flow rate of 0.535 L/min.

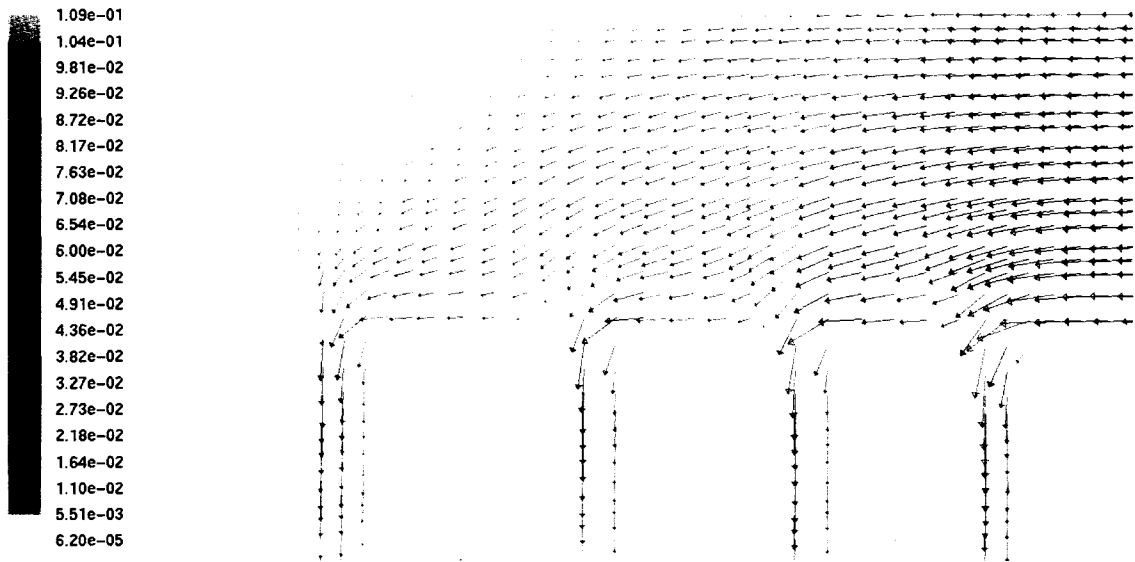


Figure 4.8 Close up of velocity vectors (m/s) entering coolant channels from the supply line on a plane taken axially through the HP-RACE target with an input volumetric flow rate of 0.535 L/min.

Fluent results using a 20 kW beam power and a volumetric flow rate in each supply line of 20 gpm (~45 L/min) showed much of the same fluid behavior. The coolant is still separated between all channels in nearly equal amounts again confirming the assumption made in the mathematical model (Figure 4.9). The higher volumetric flow rate did cause eddies when exiting the channel between the disks. This can be seen in Figures 4.10, 4.11 and 4.12. These areas could develop hotspots causing boiling of the coolant and failure of the target.

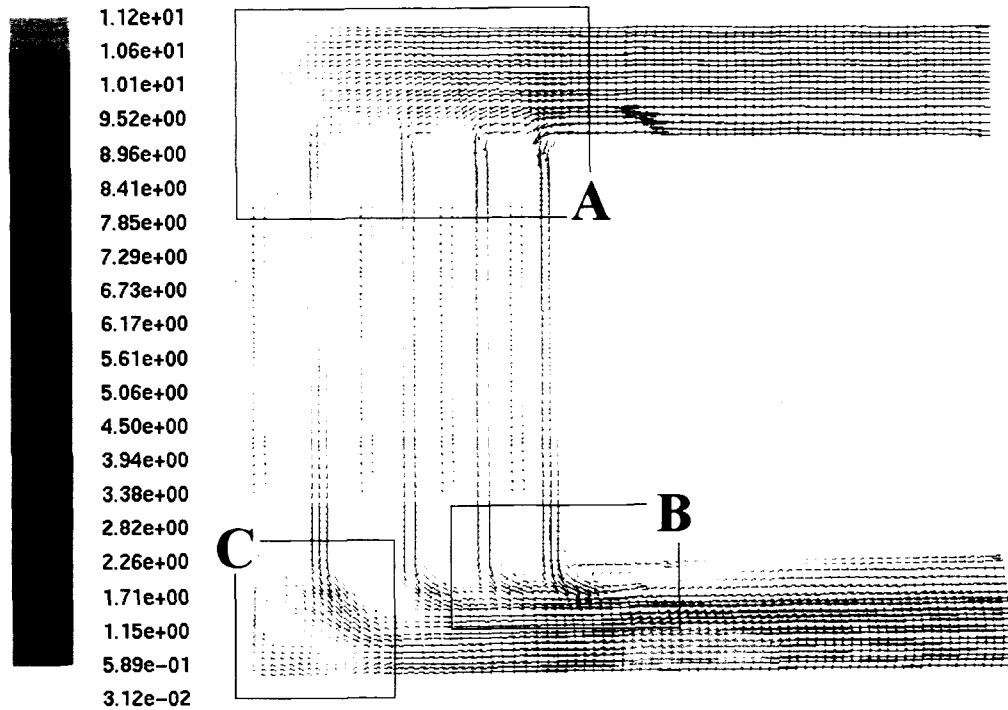


Figure 4.9 Velocity vectors (m/s) on a plane taken axially through the HP-RACE target with an input volumetric flow rate of  $\sim 45$  L/min. Boxed sections A, B, and C are detailed sections of velocity vectors shown in Figures 4.10, 4.11, and 4.12.

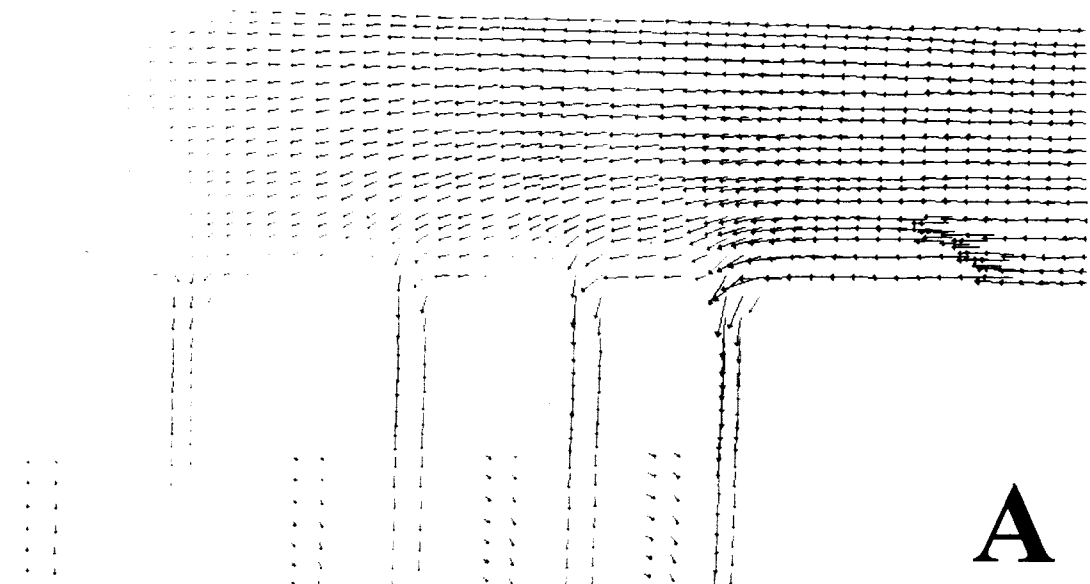
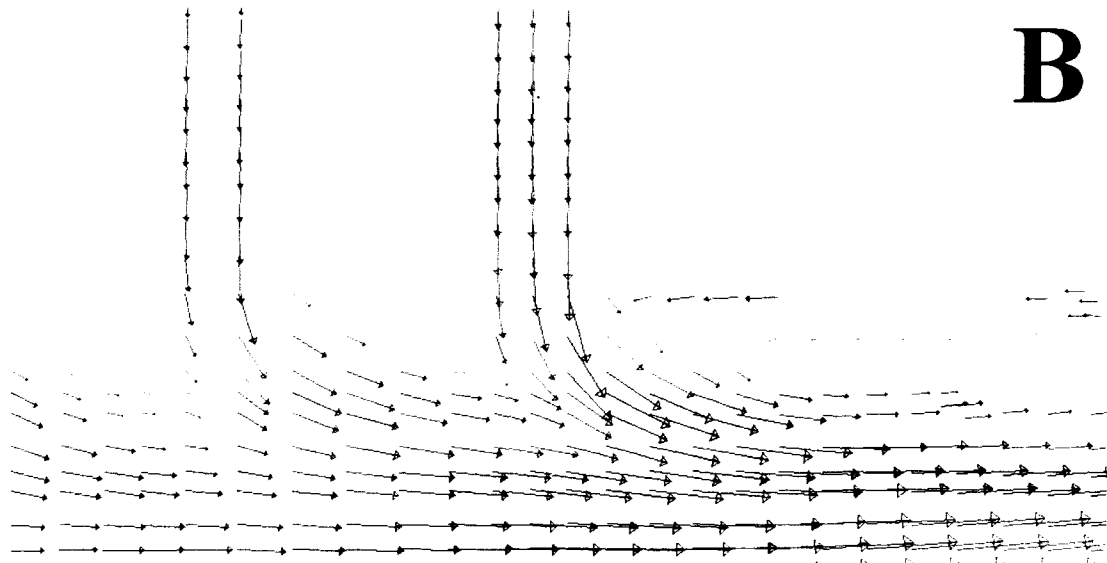
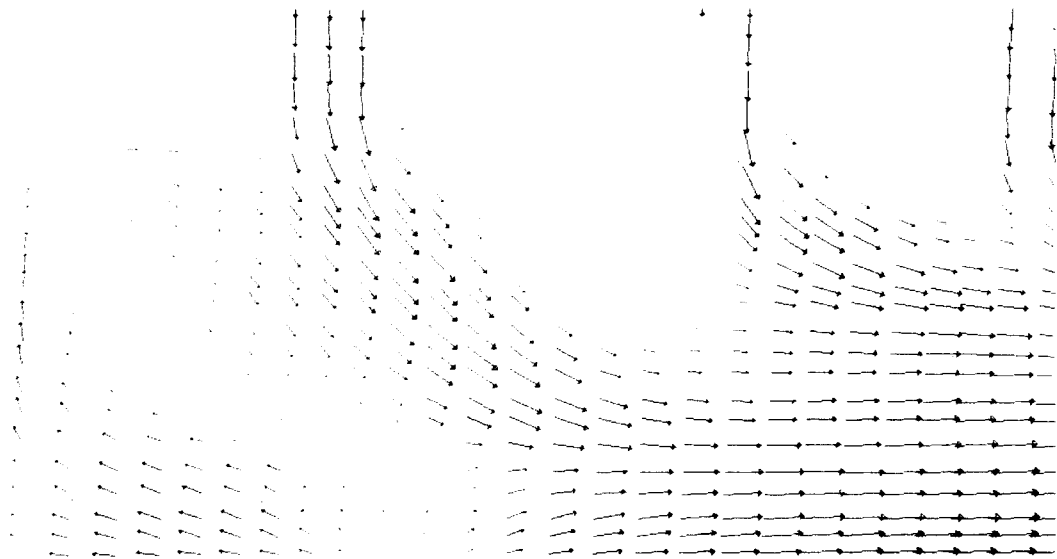


Figure 4.10 Closeup of velocity vectors (m/s) entering coolant channels from the supply line on a plane taken axially through the HP-RACE target with an input volumetric flow rate of  $\sim 45$  L/min. The flow entering the channels from the inlet coolant line has not formed any eddies.



**B**

Figure 4.11 Closeup of velocity vectors (m/s) exiting coolant channels on a plane taken axially through the HP-RACE target with an input volumetric flow rate of ~45 L/min. The formation of eddies can be seen on both sides of each channel where the coolant is entering the outlet coolant line.



**C**

Figure 4.12 Closeup of velocity vectors (m/s) exiting the rear most coolant channel on a plane taken axially through the HP-RACE target with an input volumetric flow rate of ~45 L/min. The development of eddies can be seen on the left side of the figure. This is the rear of the outlet coolant line where it ends in the target.



Velocity vectors in the center of the channels show a slightly greater flow at the edges and a slower flow in the center as was seen in the lower flow case. Figure 4.13 displays velocity vectors through the channel which display no formation of eddies. This is the area where the beam power is deposited and is of the most concern since a large amount of the power removed from the target will be removed from here.

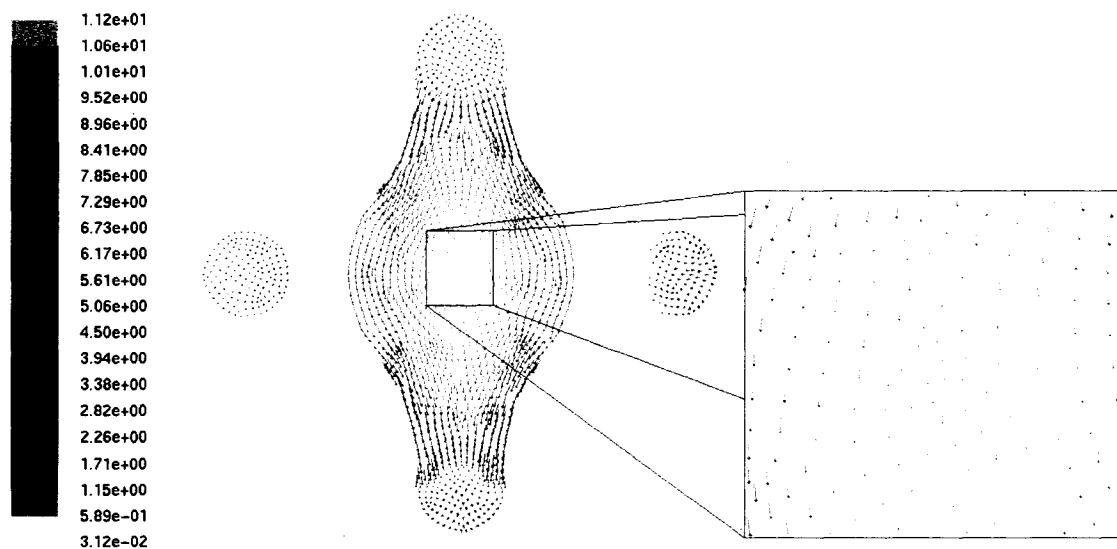


Figure 4.13 Velocity vectors (m/s) on a plane taken perpendicular to the HP-RACE Target's axis through a water channel with an input volumetric flow rate of ~45 L/min.

Temperatures were predicted to increase a maximum of about 127 K in the tungsten disks and about 3 K from the coolant inlet to the outlet (Figure 4.14). These estimates are slightly less than the calculated values of 151.4 K and 3.2 K which was expected based on the outcome of the low power results.

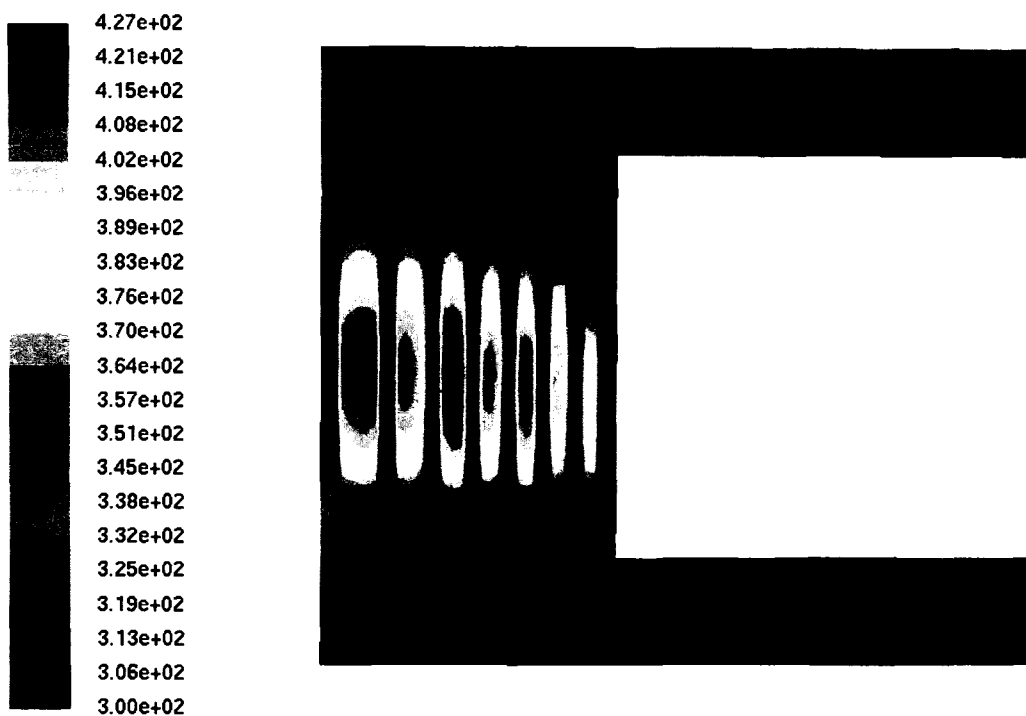


Figure 4.14 Slice taken axially through the HP-RACE Target's tungsten disk stack and cooling system showing temperature contours (K) with a 20 kW beam power.

## CHAPTER 5

### SUMMARY, CONCLUSIONS, AND RECOMMENDATIONS

#### Discussion of Results

When comparing the calculations and experimental data the differences were as expected. The experimental data showed temperature changes lower than the mathematical model predictions. This is because the coolant does not carry all of the power away from the target as assumed in the development of the mathematical model. Convective losses from the surfaces of the target, conduction to the coolant piping, insulation, and spacers the target was sitting on all contribute to the dissipation of the power absorbed in the target. In addition, there are beam power losses due to electrons that don't completely deposit all of their energy in the target and energy carried away by the high-energy x-rays and neutrons that the target is producing.

Fluent models predicted ~19% greater coolant temperature changes than those recorded during the experiment. These estimates, while remaining conservative, are more accurate than the calculations which overestimated coolant temperature changes by ~34%. This was an expected outcome since the Fluent model used many of the same assumptions the mathematical model used but evaluated the fluid and fluid flow properties through the channels as temperature changed in the disks and coolant. This resulted in conservative

estimates that were more accurate than the calculations when compared to experimental results.

Fluent also gave insight into the coolant flow through the target. Flow velocity predictions through the coolant channels agree well with the mathematical model with relative errors of less than 9% in both the low and high volumetric flow rate tests confirming the assumptions made in the mathematical model development. Eddies and possible stagnation zones were not an issue at low flow rates but were identified when high flow was present. More data is required from the interior of the coolant system to verify these results.

High power Fluent estimates for the temperature difference between the inlet and outlet were about 6% lower than calculated values. Temperature changes on the disk surfaces were also slightly lower with a maximum of ~127 K versus the ~151 K that was calculated. Though these values are greater than the boiling point of the coolant, they are not unreasonable and many steps can be taken to reduce their magnitude. Increasing coolant flow is a possibility but will be limited by the size of the coolant channels. A more logical approach would be to deposit the electron beam over the entire surface of the cooling channel. This can be done relatively easily and would reduce the surface flux of the disks to about 1/3 of its present value.

### Conclusions and Recommendations for Further Study

The mathematical and Fluent models generated conservative estimates of temperature changes in the coolant and the tungsten disks for the low power

model as expected. High power estimates from both calculations and Fluent were also reasonable. A few easily incorporated changes are required to reduce the disk surface temperature estimates.

Before full power testing is performed, further study should be done in many areas of the HP-RACE target. Since the disk surface temperatures are the determining factor in how much power can be applied to the target, verification of the power distribution among the disks should be verified. This was an assumption made in the development of the mathematical models. Accomplishing this could also verify the surface temperature estimation given by the mathematical model.

Once verification of the power distribution is made, testing at higher powers and higher flow rates should also be performed. Data at higher powers and flow rates could prove to be useful in detecting problems with coolant flow. The possibility of a blockage in a coolant channel should also be considered. A scenario such as this could have devastating consequences if it is undetected.

Finally, Fluent modeling should be revisited. A complete model of the entire target taking convection from the outside surface and conduction throughout the target into account would produce more accurate estimations. A more accurate model can not only help predict issues before they become problematic but it can help diagnose issues that arise and make understanding why those problems occurred easier.

## APPENDIX I

### DATA

#### Data Recorded During the First 30 Seconds of the 640 W Experiment

Time (s)	Inlet Temperature (°C)	Outlet Temperature (°C)	Bias (°C)	Outlet Temperature Corrected Using Average Bias (°C)	Flow Rate (L/min)
1	20.6349	21.9756	1.3407	20.6627	0.9944
2	20.6027	21.9836	1.3809	20.6707	0.9909
3	20.9001	21.9035	1.0033	20.5906	0.9938
4	20.5786	21.9836	1.4050	20.6707	0.9918
5	20.6831	21.9035	1.2203	20.5906	0.9934
6	20.3454	21.9115	1.5661	20.5986	0.9899
7	20.6912	21.9115	1.2203	20.5986	0.9938
8	20.3051	21.8874	1.5823	20.5745	0.9939
9	20.6751	21.8634	1.1883	20.5505	0.9970
10	20.2810	21.8393	1.5583	20.5264	0.9920
11	20.6992	21.9035	1.2043	20.5906	0.9938
12	20.9564	21.7992	0.8428	20.4863	0.9951
13	20.7153	21.8714	1.1561	20.5585	1.0668
14	20.4660	21.9676	1.5016	20.6547	1.0799
15	20.2327	21.8473	1.6146	20.5344	1.0917
16	20.5384	21.8072	1.2688	20.4943	1.1056
17	20.3615	21.8794	1.5180	20.5665	1.0854
18	20.6751	21.8634	1.1883	20.5505	1.0814
19	20.8037	21.7752	0.9715	20.4623	1.1129
20	20.3212	21.8473	1.5261	20.5344	1.0919
21	20.8278	21.7832	Bias Averaged Over First 20 Data Points (°C)	20.4703	1.0836
22	20.6188	21.8473		20.5344	1.0713
23	20.5625	21.7591		20.4462	1.0930
24	20.1040	21.8874		20.5745	1.0737
25	20.5786	21.9916		20.6788	1.0729
26	20.2971	21.9596		20.6467	1.0673
27	20.5062	22.0718	1.3129	20.7589	1.0954
28	20.7555	22.0878		20.7750	1.0869
29	20.5304	22.1840		20.8711	1.0956
30	20.4419	22.1439		20.8311	1.0793

## Fluent Inputs

<b>Properties of Materials Used in the Fluent Model</b>
---

<b>Water (H<sub>2</sub>O) <sup>a</sup></b>
--

Density ( $\rho$ )	998.2	kg/m <sup>3</sup>
Specific Heat ( $C_p$ )	4182	J/kg-K
Thermal Conductivity ( $k$ )	0.6	W/m-K
Viscosity ( $\mu$ )	0.001003	kg/m-s

<b>Aluminum (Al) <sup>a</sup></b>
-----------------------------------

Density ( $\rho$ )	2719	kg/m <sup>3</sup>
Specific Heat ( $C_p$ )	871	J/kg-K
Thermal Conductivity ( $k$ )	202.4	W/m-K

<b>Copper-Tungsten (Cu-W) <sup>b</sup></b>
--

Density ( $\rho$ )	14840	kg/m <sup>3</sup>
Specific Heat ( $C_p$ )	192	J/kg-K
Thermal Conductivity ( $k$ )	220	W/m-K

Notes:

a - Fluent Library

b - MatWeb Data Sheet, CMW Inc., CMW THERMKON® 83  
(25 wt% Cu, 75 wt% W)

## Source Terms Used in the Fluent Model

Radius of electron beam = 0.01625 m  
 Area beam is deposited over = 0.000829577 m<sup>2</sup>

640 W			
Volumetric Flow Rate =			0.535 l/min
Power =	640	W	0.07 m/s
Disk #	Disk Thickness (m)	Assumed W/disk	W/m <sup>3</sup>
1	0.0012	91.4	91842582
2	0.0013	91.4	84777768
3	0.0015	91.4	73474066
4	0.0018	91.4	61228388
5	0.0022	91.4	50095954
6	0.0029	91.4	38003827
7	0.0041	91.4	26880756

Full Power Estimates, 20 kW			
Volumetric Flow Rate =			12 gpm
Power =	20000	W	5.976 m/s
Disk #	Disk Thickness (m)	Assumed W/disk	W/m <sup>3</sup>
1	0.0012	2857.1	2870080687
2	0.0013	2857.1	2649305249
3	0.0015	2857.1	2296064550
4	0.0018	2857.1	1913387125
5	0.0022	2857.1	1565498557
6	0.0029	2857.1	1187619595
7	0.0041	2857.1	840023616



## BIBLIOGRAPHY

1. T. Beller, B. Howard, R. LeCounte, and D. Beller, "High-Power Accelerator Target Design for the AFCI RACE Project," *Proceedings of the 2006 International High Level Radioactive Waste Management Conference*, Las Vegas, NV, pp. 1244-1246 (2006). (Available on CD-ROM from the American Nuclear Society).
2. D. Beller, "AFCI Reactor-Accelerator Coupling Experiments (RACE) Project", AFCI Semiannual Technical Review, Idaho State University, Idaho Accelerator Center (September 13, 2004)
3. D. Beller, "Overview of the AFCI Reactor-Accelerator Coupling Experiments (RACE) Project," *Proceedings of the Eighth Information Exchange Meeting on Actinide and Fission Product Partitioning & Transmutation*, OECD/NEA, Paris, France, pp 495-504 (2005).
4. *Fluent*<sup>®</sup>, Version 6.2.16, Lebanon, NH
5. James E. Turner, *Atoms, Radiation, and Radiation Protection*, United States: John Wiley and Sons, 1995.
6. Frank P. Incropera and David P. Dewitt, *Introduction to Heat Transfer*, United States: John Wiley and Sons, 2002.
7. Michael J. Moran and Howard N. Shapiro, *Fundamentals of Engineering Thermodynamics*, United States: John Wiley and Sons, 2004.
8. Partitioning and Transmutation: Making Wastes Nonradioactive. Oak Ridge National Laboratory. 30 March 1998.
9. Gohar, Y., "Design and Analyses of Electron Tungsten Targets for Neutron Generation", presented at the Fourth Annual ADSS Experiments Workshop, Texas A&M University on 11-14 April 2006.
10. LeCounte, R., Beller, T., Howard B., Beller, D., and Cook, D., "Design of the High-Power RACE Target," *Proceedings of the Eighth International Topical Meeting on Nuclear Applications and Utilization of Accelerators*, 30 July-2 August 2007, Pocatello, Idaho.

## VITA

Graduate College  
University of Nevada, Las Vegas

Ryan Dean LeCounte

### Home Address:

6105 Kitamaya St.  
North Las Vegas, NV

### Degrees:

Bachelor of Science in Mechanical Engineering, 2006  
University of Nevada, Las Vegas

### Publications:

LeCounte, R.D., Beller, T.E., Howard B., Beller, D.E., and Cook, D., "Design of the High-Power RACE Target," *Proceedings of the Eighth International Topical Meeting on Nuclear Applications and Utilization of Accelerators*, 30 July-2 August 2007, Pocatello, Idaho.

T. Beller, B. Howard, R. LeCounte, and D. Beller, "High-Power Accelerator Target Design for the AFCI RACE Project," *Proceedings of the 2006 International High Level Radioactive Waste Management Conference*, Las Vegas, NV, pp. 1244-1246 (2006). (Available on CD-ROM from the American Nuclear Society).

Thesis Title: Thermal Hydraulic Analysis of the High-Power RACE Target

### Thesis Examination Committee:

Chairperson, Dr. Daniel Cook, Ph. D.  
Committee Member, Dr. Charlotta Sanders, Ph. D., P.E.  
Committee Member, Dr. Denis Beller, Ph. D.  
Graduate Faculty Representative, Dr. Julie Staggers, Ph. D.